I S A V

Journal of Theoretical and Applied Vibration and Acoustics

journal homepage: http://tava.isav.ir

A finite element model for extension and shear modes of piezo-laminated beams based on von Karman's nonlinear displacement-strain relation

Ahmad Ali Tahmasebi Moradi, Saeed Ziaei-Rad, Reza Tikani *, Hamid Reza Mirdamadi

Department of Mechanical Engineering, Isfahan University of Technology, Isfahan 84156-83111, Iran

ARTICLE INFO

Article history:
Received 29 July 2015

Received in revised form
1 January 2016

Accepted 15 March 2016

Available online 1 April 2016

Keywords:
Piezolaminated sandwich beam

Finite element model

von Karman's relation

Third-order shear deformation theory

ABSTRACT

Piezoelectric actuators and sensors have been broadly used for design of smart structures over the last two decades. Different theoretical assumptions have been considered in order to model these structures by the researchers. In this paper, an enhanced piezolaminated sandwich beam finite element model is presented. The facing layers follow the Euler-Bernoulli assumption while the core layers are modeled with the third-order shear deformation theory (TSDT). To refine the model, the displacement-strain relationships are developed by using von Karman's nonlinear displacement-strain relation. It will be shown that this assumption generates some additional terms on the electric fields and also introduces some electromechanical potential and non-conservative work terms for the extension piezoelectric sub-layers. A variational formulation of the problem is presented. In order to develop an electromechanically coupled finite element model of the extension/shear piezolaminated beam, the electric DoFs as well as the mechanical DoFs are considered. For computing the natural frequencies, the governing equation is linearized around a static equilibrium position. Comparing natural frequencies, the effect of nonlinear terms is studied for some examples.

1. Introduction

Piezoelectric actuators/sensors have been widely used for design of smart structures over the last two decades leading to high-performance and light-weight solutions. They can be either surface-mounted or embedded into a host structure. Surface-mounted actuators/sensors are normally poled in the thickness direction, so that they act as extension actuators/sensors, while embedded actuators/sensors are normally poled in the longitudinal direction; therefore, they act as shear actuators/sensors.

* Corresponding Author: Reza Tikani, Email: r_tikani@cc.iut.ac.ir

In view of their wide application, the modeling of these structures is a major concern for many researchers. It often requires a coupled modeling between the host structure and the piezoelectric sensors and actuators. Due to the complexity of these systems, different theoretical assumptions have been considered in order to deal with the coupling effect between the mechanical and electric fields and thus, considerable research has been carried out in this regard [1-4]. Most of the existing refined models for piezolaminate structures focus on extension piezoelectric actuators and sensors [5-7]. Since extension actuators present a simpler electrical behavior, simple low order electric models with higher order mechanical models have been developed more commonly.

On the other hand, piezolaminated beam models based on the equivalent single layer (ESL) theory cannot accurately model the local shear deformation of the embedded piezoelectric shear sensors/actuators [8]. As a result, calculations of both deflections induced by piezoelectric actuators and induced electric potential on piezoelectric shear sensors by structural deflection are obstructed [9]. Thus, using the classical sandwich beam theory presents a proper mathematical approach for modeling the structures with piezoelectric shear layers in order to analyze the system statically and dynamically [9-13]. A shear locking free electromechanically coupled finite element model for a multilayer beam consisting of both extension and shear piezoelectric layers was proposed by Trinidade et al. [11]. In this work, the Euler–Bernoulli hypothesis was assumed for the face sub-layers where the Timoshenko theory was considered for the core layer. Later, the electric DoFs were introduced as well as the mechanical DoFs leading to a finite element model which was in a proper form considering the controller design viewpoint [10-12]. To provide a better model, the third-order shear deformation theory (TSDT) was used for the core layer instead of the Timoshenko first order shear deformation theory (FSDT) [9]. Also, a static finite element model was proposed for the piezoelectric sandwich beam and a third-order electric potential was considered for the core piezoelectric layer due to considering the TSDT. As a result, more realistic presentations for both shear strain and core electric field were achieved and it was shown that using the TSDT could lead to more accurate results of 10-20% for the corresponding cases. In a later modeling effort [13], a dynamic finite element model was presented where mechanical and electric DoFs were grouped differently to provide a better understanding of the electric boundary conditions.

In this paper, an improved piezolaminated sandwich beam model is presented. The facing layers follow the Euler-Bernoulli assumption while the core layers are modeled with the third-order shear deformation theory (TSDT). To refine the model, the displacement-strain relationships are developed using the von Karman's nonlinear displacement-strain relation. It will be shown that this assumption generates some additional terms on the electric fields and also introduces some electromechanical potential and non-conservative work terms for the extension piezoelectric sub-layers. A variational formulation of the problem is presented. The electromechanically coupled finite element model of the piezolaminated beam was incorporating both the electric and the mechanical DoFs. The governing equation is linearized around a static equilibrium position to compute the natural frequencies. Using modal analysis, it is shown that the obtained results are in a good agreement with the available data in the literature. Finally, it is shown that if the output voltage of the extension piezoelectric layer is taken as the sensor signal, the governing equation of the system will be nonlinear. In case of fairly high deformation, this nonlinearity will be more noticeably effective and causes the natural flexural frequencies to behave erratically.

2. Theoretical formulation

The proposed model is considering a multilayer beam made of piezoelectric layers using the classical sandwich theory. The piezolaminated beam consists of a core layer sandwiched between top and bottom laminate face layers. The core itself consists of piezoelectric and elastic materials. The Euler-Bernoulli theory is assumed for the extension piezoelectric face layers; therefore, they are modeled using classical laminate theory. On the contrary, the core layer undergoes the shear strains; hence, it is modeled using the TSDT proposed by [14]. For simplicity, all piezoelectric layers are assumed to be orthotropic perfectly either bonded or embedded and in the plane stress state. Also, the extension piezoelectric face layers are poled in the thickness direction, while the shear piezoelectric layer is poled in the longitudinal direction. The length, width and thickness of the beam are denoted by L, b and h respectively. Quantities which are related to the upper, core and lower layers are represented by the subscripts a_j, c and b_j where the set of subscript $j=\{1,\ldots,(n,m)\}$ denotes a sub-layer of the laminate faces. Faces a and b may have n and m sub-layers respectively.

2.1. Kinematics and strains

In view of the aforementioned assumptions, the axial and transverse displacement fields of the core and face layers are written as follows (see Fig. 1):

$$\breve{u}_k(x,y,z,t)=u_k(x,t)+(z-z_k)\beta_k(x,t);\quad k=a,b$$

$$\breve{u}_c(x,y,z,t)=u_c(x,t)+(z-z_c)\beta_c(x,t)-\frac{4(z-z_c)^3}{3h_c^2}\left[\beta_c(x,t)+w(x,t)'\right]; \tag{1}$$

$$\breve{w}_i(x,y,z,t)=w(x,t);\quad i=a,b,c$$

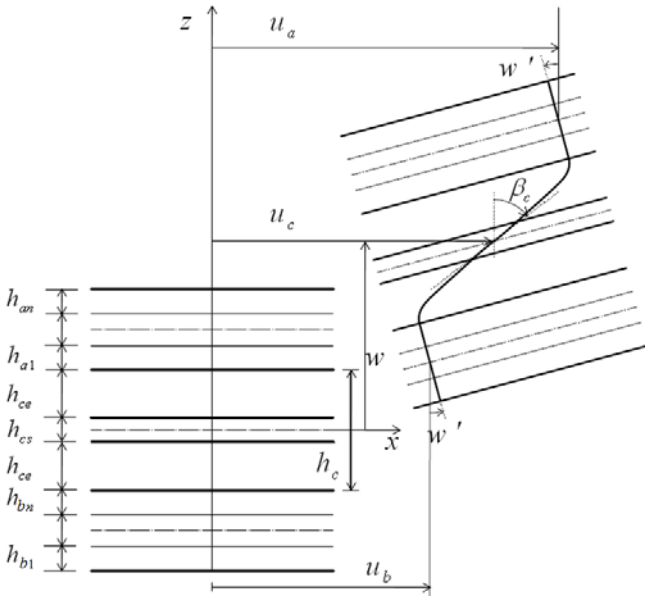

Fig. 1. Kinematic representation of the piezolaminated beam

where u_l is the axial displacement, β_l is the transverse normal rotation, z_l is the local z-axis and w is the transverse displacement, whereas $l = a,b,c$.

The same displacement fields $u_k\,(k = a,b)$ are presumed for all the face sub-layers k_j of the face k . Based on the Euler-Bernoulli theory, $\beta_k = -w'$. For the sake of simplicity, the mid-plane of the core is set to coincide with the origin of z-axis, namely $z_c = 0$. In the following sections, the arguments *y* and *t* will be ignored for notational simplicity.

Applying the displacement continuity conditions between the layers, the displacement field of Eq. (1) can be written in terms of the three main variables u_c , β_c and w as follows:

$$\breve{u}_k(x,z) = \left(u_c \pm \frac{h_c \beta_c}{3} \mp d_k w'\right) - (z - z_k)w'; \quad k = a(+),b(-)$$

$$\breve{u}_c(x,z) = u_c + z\,\beta_c - \frac{4z^3}{3h_c^2}(\beta_c + w') \tag{2}$$

$$\breve{w}_i(x,z) = w(x); \qquad i = a,b,c$$

where

$$d_k = \frac{3h_k + h_c}{6};\; z_k = \pm\frac{h_k + h_c}{2};\; h_k = \sum_{j=1}^{n,m} h_{k_j} \quad k = a(+,n),b(-,m)$$

$$h_c = 2h_{ce} + h_{cs} \tag{3}$$

Using the von Karman's nonlinear displacement-strain relation, the axial ε_1 and shear ε_5 strains for the i^{th} layer are written as:

$$\varepsilon_{1k} = \varepsilon_k^m + (z - z_k)\varepsilon_k^b + \frac{1}{2}\varepsilon_t^2$$

$$\varepsilon_{1c} = \varepsilon_c^m + z\,\varepsilon_c^b - \frac{4z^3}{3h_c^2}\varepsilon_c^h + \frac{1}{2}\varepsilon_t^2 \tag{4}$$

$$\varepsilon_{5c} = \left(1 - \frac{4z^2}{h_c^2}\right)\varepsilon_c^s$$

where

$$\varepsilon_k^m = \left(u_c' \pm \frac{h_c \beta_c'}{3} \mp d_k w''\right);\; \varepsilon_k^b = -w'';\; k = a(+),b(-)$$

$$\varepsilon_c^m = u_c';\; \varepsilon_c^b = \beta_c';\; \varepsilon_c^h = \beta_c' + w'';\; \varepsilon_c^s = \beta_c + w';\; \varepsilon_t = w' \tag{5}$$

2.2. Reduced piezoelectric constitutive equations

Linear orthotropic piezoelectric materials which have the material symmetry axes parallel to the beam ones are considered here. Parameters c_{ij} , e_{kj} and ε_{kk} $(i, j = 1,\ldots,6; k = 1,2,3)$ represent the elastic, piezoelectric and dielectric material constants respectively.

The extension piezoelectric layers are poled transversely and subjected to the transverse and longitudinal electric fields. This assumption is considered to satisfy the equilibrium electrostatic equation due to the von Karman's displacement-strain relation. Thus, the three dimensional linear constitutive equations of the extension piezoelectric face layers due to the plane stress assumption ($\sigma_3 = 0$) can be reduced to:

$$\begin{Bmatrix} \sigma_{1k_j} \\ D_{1k_j} \\ D_{3k_j} \end{Bmatrix} = \begin{bmatrix} c_{11}^{k_j^*} & 0 & -e_{31}^{k_j^*} \\ 0 & \in_{11}^{k_j} & 0 \\ e_{31}^{k_j^*} & 0 & \in_{33}^{k_j^*} \end{bmatrix} \begin{Bmatrix} \varepsilon_{1k} \\ E_{1k_j} \\ E_{3k_j} \end{Bmatrix} \tag{6}$$

where

$$c_{11}^{k_j^*} = c_{11}^{k_j} - \frac{{c_{13}^{k_j}}^2}{c_{33}^{k_j}}; \qquad e_{31}^{k_j^*} = e_{31}^{k_j} - \frac{c_{13}^{k_j}}{c_{33}^{k_j}} e_{33}^{k_j}; \qquad \in_{33}^{k_j^*} = \in_{33}^{k_j} + \frac{{e_{33}^{k_j}}^2}{c_{33}^{k_j}} \tag{7}$$

σ_{1k_j} , ε_{1k_j} , D_{1k_j} , E_{1k_j} , D_{3k_j} and E_{3k_j} are the axial stress, strain, longitudinal electric displacement, longitudinal electric field, transverse electric displacement and transverse electric field respectively. Sub-script k_j is related to the face piezoelectric layers (or extension piezoelectric layers as their second name).

The piezoelectric core layers are poled in the longitudinal direction. Therefore, the three dimensional linear constitutive equations due to the plane stress assumption ($\sigma_3 = 0$) can be reduced to:

$$\begin{Bmatrix} \sigma_{1c} \\ \sigma_{5c} \\ D_{1c} \\ D_{3c} \end{Bmatrix} = \begin{bmatrix} c_{33}^{c^*} & 0 & -e_{33}^{c^*} & 0 \\ 0 & c_{55}^{c} & 0 & -e_{15}^{c} \\ e_{33}^{c^*} & 0 & \in_{33}^{c^*} & 0 \\ 0 & e_{15}^{c} & 0 & \in_{11}^{c} \end{bmatrix} \begin{Bmatrix} \varepsilon_{1c} \\ \varepsilon_{5c} \\ E_{1c} \\ E_{3c} \end{Bmatrix} \tag{8}$$

where

$$c_{33}^{c^*} = c_{33}^{c} - \frac{{c_{13}^{c}}^2}{c_{11}^{c}}; \qquad e_{33}^{c^*} = e_{33}^{c} - \frac{c_{13}^{c}}{c_{11}^{c}} e_{31}^{c}; \qquad \in_{33}^{c^*} = \in_{33}^{c} + \frac{{e_{31}^{c}}^2}{c_{11}^{c}} \tag{9}$$

σ_{5c} and ε_{5c} are the transverse shear stress and strain respectively. Sub-script c is pertaining to the core piezoelectric layer.

2.3. Electric potentials and fields

For the extension piezoelectric layers, both transverse and longitudinal electric fields are presumed. Furthermore, it is assumed that the transverse electric field is linear through the

thickness. Therefore, the electric potential in the extension piezoelectric layers is considered to be quadratic such as:

$$\psi_{k_j}(x,z) = \psi_{0_j}(x) + \frac{z}{h_{k_j}}\psi_{1_j}(x) + \frac{z^2}{h_{k_j}^2}\psi_{2_j}(x) \tag{10}$$

Applying the electric boundary conditions on the upper and lower skins of the face piezoelectric layers yields:

$$\begin{aligned} \psi_{k_j}(x, z_{k_j} + \frac{h_{k_j}}{2}) &= \psi_{k_j}^{+} \\ \psi_{k_j}(x, z_{k_j} - \frac{h_{k_j}}{2}) &= \psi_{k_j}^{-} \end{aligned} \tag{11}$$

By the following definitions,

$$\begin{aligned} V_{k_j} &= \psi_{k_j}^{+} - \psi_{k_j}^{-} \\ \psi_{mk_j} &= \frac{\psi_{k_j}^{+} + \psi_{k_j}^{-}}{2} \end{aligned} \tag{12}$$

the following relationship can be obtained:

$$\begin{aligned} \psi_{1_j} + \frac{2z_{k_j}}{h_{k_j}}\psi_{2_j} &= V_{k_j} \\ \psi_{0_j} + \frac{z_{k_j}}{h_{k_j}}\psi_{1_j} + \frac{\left(z_{k_j}^2 + \frac{h_{k_j}^2}{4}\right)}{h_{k_j}^2}\psi_{2_j} &= \psi_{mk_j} \end{aligned} \tag{13}$$

For an extension piezoelectric patch with its upper and lower skins covered completely by electrodes, the electric potential $\psi_{k_j}^{+}$ and $\psi_{k_j}^{-}$, or equivalently, V_{k_j} and ψ_{mk_j}, are constants in the longitudinal direction. Thus, the electric potential (Eq. (10)) can be rewritten as follows:

$$\psi_{k_j}(x,z) = \psi_{mk_j} + \frac{\left(z - z_{k_j}\right)}{h_{k_j}}V_{k_j} + \left[\frac{(z - z_{k_j})^2 - \frac{h_{k_j}^2}{4}}{h_{k_j}^2}\right]\psi_{2_j}(x) \tag{14}$$

Hence, the axial $E_{1k_j} = -\partial\psi_{k_j}/\partial x$ and the transverse $E_{3k_j} = -\partial\psi_{k_j}/\partial z$ electric fields are expressed as:

$$E_{1k_j} = -\left[\frac{(z - z_{k_j})^2 - \frac{h_{k_j}^2}{4}}{h_{k_j}^2}\right]\psi'_{2_j}(x) \tag{15}$$

$$E_{3k_j} = -\frac{V_{k_j}}{h_{k_j}} - \left[\frac{2(z - z_{k_j})}{h_{k_j}^2}\right]\psi_{2_j}(x)$$

As noted in Eq. (15), the longitudinal electric field appears only due to considering the electric potential higher-order terms. Moreover, it vanishes on the upper and lower skins of extension piezoelectric layers (see Eq. (15)). By solving the following electrostatic equilibrium equation, the choice of a quadratic electric potential is justified.

$$D_{1k_j,1} + D_{2k_j,2} + D_{3k_j,3} = 0 \tag{16}$$

Assuming $D_{2k_j,2} = 0$ and substituting Eq. (6) into the previous equation leads to:

$$\in_{11}^{k_j} \frac{\partial E_{1k_j}}{\partial x} + e_{31}^{k_j^*} \frac{\partial \varepsilon_{1k}}{\partial z} + \in_{33}^{k_j^*} \frac{\partial E_{3k_j}}{\partial z} = 0 \tag{17}$$

This equation must be satisfied in each point along the z direction. Using Eqs. (4) and (15), the previous equation results into the following equations:

$$-\in_{11}^{k_j} \frac{z_{k_j}^2}{h_{k_j}^2}\psi''_{2_j} + \frac{\in_{11}^{k_j}}{4}\psi''_{2_j} - e_{31}^{k_j^*} w'' - \frac{2 \in_{33}^{k_j^*}}{h_{k_j}^2}\psi_{2_j} = 0$$

$$\frac{2 \in_{11}^{k_j} z_{k_j}}{h_{k_j}^2}\psi''_{2_j} = 0 \tag{18}$$

$$-\frac{\in_{11}^{k_j}}{h_{k_j}^2}\psi''_{2_j} = 0$$

Obviously, ψ_{2_j} depends only on w . ψ_{2_j} and its second derivative are obtained as follows:

$$\psi''_{2_j} = 0$$

$$\psi_{2_j} = -\frac{e_{31}^{k_j^*} h_{k_j}^2}{2 \in_{33}^{k_j^*}} w'' \tag{19}$$

Finally, the longitudinal and transverse electric fields can be expressed in the following forms:

$$E_{1k_j} = -\frac{\partial \psi_{k_j}}{\partial x} = \left[(z - z_{k_j})^2 - \frac{h_{k_j}^2}{4}\right]\frac{e_{31}^{k_j^*}}{2 \in_{33}^{k_j^*}} w'''$$

$$E_{3k_j} = -\frac{\partial \psi_{k_j}}{\partial z} = -\frac{V_{k_j}}{h_{k_j}} + (z - z_{k_j})\frac{e_{31}^{k_j^*}}{\in_{33}^{k_j^*}} w'' \tag{20}$$

or alternatively,

$$E_{1k_j} = -\frac{\partial \psi_{k_j}}{\partial x} = -\left[(z - z_{k_j})^2 - \frac{h_{k_j}^2}{4}\right]\frac{e_{31}^{k_j^*}}{2 \in_{33}^{k_j^*}} \varepsilon_k^{b\prime}$$

$$E_{3k_j} = -\frac{\partial \psi_{k_j}}{\partial z} = -\frac{V_{k_j}}{h_{k_j}} - (z - z_{k_j})\frac{e_{31}^{k_j^*}}{\in_{33}^{k_j^*}} \varepsilon_k^b \tag{21}$$

It is worth mentioning that in the case of assuming small deformation domain, the von Karman's displacement-strain relation, doesn't impose any effect on the electric fields for the extension piezoelectric layers.

For the shear piezoelectric layer, the same strategy is applied. Both longitudinal and transverse electric fields are considered here. In addition, a quadratic variation through the thickness is assumed for the transverse electric field, i.e., the electric potential in the core piezoelectric layers follows cubic variations across the thickness presented with the following equation:

$$\psi_c(x,z) = \psi_0(x) + \frac{z}{h_{cs}}\psi_1(x) + \frac{z^2}{h_{cs}^2}\psi_2(x) + \frac{z^3}{h_{cs}^3}\psi_3(x) \tag{22}$$

The longitudinal and transverse electric fields for the shear piezoelectric layer are expressed as follows based on [13]:

$$E_{1c} = -\frac{\partial \psi_c}{\partial x} = -\left(\frac{z^2}{h_{cs}^2} - \frac{1}{4}\right)\frac{z}{h_{cs}}\psi_3'$$

$$E_{3c} = -\frac{\partial \psi_c}{\partial z} = -\frac{V_c}{h_{cs}} - \left(\frac{3z^2}{h_{cs}^2} - \frac{1}{4}\right)\frac{\psi_3}{h_{cs}} \tag{23}$$

where electric boundary conditions on the upper and lower skins of the piezoelectric layers are the same as extension piezoelectric layers (Eq. (11)). From Eqs. (21) and (23), obviously, the independent variables for the electric fields are V_{k_j}, V_c and ψ_3.

2.4. Variational formulation

Using the Hamilton's principle with an extension for piezoelectric media, the following variational equation can be written for the multilayer beam:

$$\int_{t_1}^{t_2}\left(\delta T - \delta H + \delta W^{C}\right)dt + \int_{t_1}^{t_2}\delta W^{NC} = 0$$

$$\forall \delta u_c, \delta\beta_c, \delta w, \delta w', \delta V_{k_j}, \delta V_c, \delta\psi_3 \tag{24}$$

where T, H, W^{C} and W^{NC} are the kinetic energy, the electromechanical enthalpy, the work of conservative forces and the work of non-conservative forces respectively. The electromechanical enthalpy in the layered faces sandwich beam is,

$$H = H_{ce} + H_{cs} + \sum_{k=a}^{b}\sum_{j=1}^{n,m} H_{k_j} \tag{25}$$

where

$$H_{k_j} = \frac{1}{2}\int_{V_{k_j}} \left(\sigma_{1k_j}\varepsilon_{1k} - D_{3k_j}E_{3k_j} - D_{1k_j}E_{1k_j}\right)dv$$

$$H_{cs} = \frac{1}{2}\int_{V_{cs}} \left(\sigma_{1c}\varepsilon_{1c} + \sigma_{5c}\varepsilon_{5c} - D_{1c}E_{1c} - D_{3c}E_{3c}\right)dv \tag{26}$$

$$H_{ce} = \frac{1}{2}\int_{V_{ce}} \left(\sigma_{1c}\varepsilon_{1c} + \sigma_{5c}\varepsilon_{5c}\right)dv$$

H_{k_j} is the electromechanical enthalpy of the k_j-th extension piezoelectric layer, H_{cs} is the electromechanical enthalpy of the shear piezoelectric layers in the core and H_{ce} is the mechanical enthalpy of the elastic layer in the core.

By using the strain field relations (Eq. (4)), the constitutive relations (Eqs. (6) and (8)) and the electric field relations (Eq. (21) and (23)) while neglecting the higher-order terms such as $\varepsilon_t^2, \varepsilon_c^h\varepsilon_t, \varepsilon_c^b\varepsilon_t, \varepsilon_c^m\varepsilon_t, \varepsilon_t^3, \varepsilon_t''\varepsilon_t, \varepsilon_k^m\varepsilon_t, \varepsilon_k^b\varepsilon_t$ (considering the small deformation domain) and applying the variational operator for integration through the thickness, the previous equations result into:

$$\delta H_{k_j} = \int_0^L \left\{ \begin{array}{l} \delta\varepsilon_k^m \left[c_{11}^{k_j^*}\left(A_{k_j}\varepsilon_k^m + I_{mk_j}^{(1)}\varepsilon_k^b\right) - e_{31}^{k_j^*}\left(-A_{k_j}\dfrac{V_{k_j}}{h_{k_j}} - I_{ek_j}^{(1)}\dfrac{e_{31}^{k_j^*}}{\in_{33}^{k_j^*}}\varepsilon_k^b\right)\right] \\ +\delta\varepsilon_k^b \left[c_{11}^{k_j^*}\left(I_{mk_j}^{(1)}\varepsilon_k^m + I_{mk_j}^{(2)}\varepsilon_k^b\right) - e_{31}^{k_j^*}\left(-I_{mk_j}^{(1)}\dfrac{V_{k_j}}{h_{k_j}} - I_{mek_j}\dfrac{e_{31}^{k_j^*}}{\in_{33}^{k_j^*}}\varepsilon_k^b\right)\right] \\ +\delta\varepsilon_t \left(e_{31}^{k_j^*}A_{k_j}\dfrac{V_{k_j}}{h_{k_j}}\varepsilon_t \right) \\ +\dfrac{\delta V_{k_j}}{h_{k_j}} \left[e_{31}^{k_j^*}\left(A_{k_j}\varepsilon_k^m + I_{mk_j}^{(1)}\varepsilon_k^b\right) + \in_{33}^{k_j^*}\left(-A_{k_j}\dfrac{V_{k_j}}{h_{k_j}} - I_{ek_j}^{(1)}\dfrac{e_{31}^{k_j^*}}{\in_{33}^{k_j^*}}\varepsilon_k^b\right)\right] \\ +\delta\varepsilon_k^b \dfrac{e_{31}^{k_j^*}}{\in_{33}^{k_j^*}} \left[\begin{array}{l} e_{31}^{k_j^*}\left(I_{ek_j}^{(1)}\varepsilon_k^m + I_{mek_j}\varepsilon_k^b\right) \\ +\in_{33}^{k_j^*}\left(-\dfrac{I_{ek_j}^{(1)}V_{k_j}}{h_{k_j}} - I_{ek_j}^{(2)}\dfrac{e_{31}^{k_j^*}}{\in_{33}^{k_j^*}}\varepsilon_k^b\right) \end{array}\right] \\ -\delta\varepsilon_k'^b \dfrac{\in_{11}^{k_j} e_{31}^{k_j^*2}}{4\in_{33}^{k_j^*2}}\left(I_{ek_j}^{(3)} + \dfrac{A_{k_j}h_{k_j}^4}{16} - \dfrac{I_{ek_j}^{(2)}h_{k_j}^2}{2}\right)\varepsilon_k'^b \end{array} \right\} dx \tag{27}$$

The presence of the term $+\delta\varepsilon_t\left(e_{31}^{k_j^*}A_{k_j}\dfrac{V_{k_j}}{h_{k_j}}\varepsilon_t\right)$ is due to considering the von Karman's displacement-strain relation. It is clear that this term can be considered for extension piezoelectric sensors where the sensor signal is the output voltage. It will be shown that since this term does not vanish for sensors, the governing equation of the system will be nonlinear and thus, this term is the origin of the nonlinearity in the system.

$$\delta H_{cs}=\int_{V_{cs}}\left\{\begin{array}{l}\delta\varepsilon_c^m\left(c_{33}^{c^*}A_{cs}\varepsilon_c^m\right)\\+\delta\varepsilon_c^b\left[c_{33}^{c^*}\left(I_{cs}^{(1)}\varepsilon_c^b-\frac{4I_{cs}^{(2)}}{3h_c^2}\varepsilon_c^h\right)+\frac{e_{33}^{c^*}}{h_{cs}}\left(\frac{I_{cs}^{(2)}}{h_{cs}^2}-\frac{I_{cs}^{(1)}}{4}\right)\psi_3'\right]\\-\delta\varepsilon_c^h\left[c_{33}^{c^*}\left(\frac{4I_{cs}^{(2)}}{3h_c^2}\varepsilon_c^b-\frac{16I_{cs}^{(3)}}{9h_c^4}\varepsilon_c^h\right)+\frac{4e_{33}^{c^*}}{3h_c^2h_{cs}}\left(\frac{I_{cs}^{(3)}}{h_{cs}^2}-\frac{I_{cs}^{(2)}}{4}\right)\psi_3'\right]\\+\delta\psi_3'\left[\begin{array}{l}e_{33}^{c^*}\left(\frac{1}{h_{cs}}\left(\frac{I_{cs}^{(2)}}{h_{cs}^2}-\frac{I_{cs}^{(1)}}{4}\right)\varepsilon_c^b-\frac{4}{3h_c^2h_{cs}}\left(\frac{I_{cs}^{(3)}}{3h_{cs}^2}-\frac{I_{cs}^{(2)}}{4}\right)\varepsilon_c^h\right)\\+\in_{33}^{c^*}\left(-\left(\frac{I_{cs}^{(3)}}{h_{cs}^6}-\frac{I_{cs}^{(2)}}{2h_{cs}^4}+\frac{I_{cs}^{(1)}}{16h_{cs}^2}\right)\psi_3'\right)\end{array}\right]\\+\delta\varepsilon_c^s\left[c_{55}^c\left(A_{cs}+\frac{16I_{cs}^{(2)}}{h_c^4}-\frac{8I_{cs}^{(1)}}{h_c^2}\right)\varepsilon_c^s\right]\\-\delta\varepsilon_c^s\frac{e_{15}^c}{2}\left[-\left(A_{cs}-\frac{4I_{cs}^{(1)}}{h_c^2}\right)\frac{V_c}{h_{cs}}-\left(-\frac{12I_{cs}^{(2)}}{h_c^2h_{cs}^2}+\frac{3I_{cs}^{(1)}}{h_{cs}^2}+\frac{I_{cs}^{(1)}}{h_c^2}-\frac{A_{cs}}{4}\right)\frac{\psi_3}{h_c}\right]\\+\frac{\delta V_c}{h_{cs}}\left[\begin{array}{l}\frac{e_{15}^c}{2}\left(\left(A_{cs}-\frac{4I_{cs}^{(1)}}{h_c^2}\right)\varepsilon_c^s\right)\\+\in_{11}^c\left(-\frac{A_{cs}V_c}{h_{cs}}-\left(\frac{3I_{cs}^{(1)}}{h_{cs}^2}-\frac{A_{cs}}{4}\right)\frac{\psi_3}{h_{cs}}\right)\end{array}\right]\\+\delta\psi_3\left[\begin{array}{l}\frac{e_{15}^c}{2h_{cs}}\left(\left(-\frac{12I_{cs}^{(2)}}{h_c^2h_{cs}^2}+\frac{3I_{cs}^{(1)}}{h_{cs}^2}+\frac{I_{cs}^{(1)}}{h_c^2}-\frac{A_{cs}}{4}\right)\varepsilon_c^s\right)\\+\in_{11}^c\left(\begin{array}{l}-\frac{V_c}{h_{cs}^2}\left(\frac{3I_{cs}^{(1)}}{h_{cs}^2}-\frac{A_{cs}}{4}\right)\\-\left(\frac{9I_{cs}^{(2)}}{h_{cs}^4}-\frac{3I_{cs}^{(1)}}{2h_{cs}^2}+\frac{A_{cs}}{16}\right)\frac{\psi_3}{h_{cs}^2}\end{array}\right)\end{array}\right]\end{array}\right\}dv \tag{28}$$

$$\delta H_{ce}=\int_0^L\left\{\begin{array}{l}\delta\varepsilon_c^m c_{11}^{ce}A_{ce}\varepsilon_c^m+\delta\varepsilon_c^b c_{11}^{ce}\left(I_{ce}^{(1)}\varepsilon_c^b-\frac{4I_{ce}^{(2)}}{3h_c^2}\varepsilon_c^h\right)\\-\delta\varepsilon_c^h c_{11}^{ce}\left(\frac{4I_{ce}^{(2)}}{3h_c^2}\varepsilon_c^b-\frac{16I_{ce}^{(3)}}{9h_c^4}\varepsilon_c^h\right)\\+\delta\varepsilon_c^s\left[c_{55}^{ce}\left(A_{ce}+\frac{16I_{ce}^{(2)}}{h_c^4}-\frac{8I_{ce}^{(1)}}{h_c^2}\right)\varepsilon_c^s\right]\end{array}\right\}dx \tag{29}$$

where

$$\left[A_{k_j},I_{mk_j}^{(1)},I_{mk_j}^{(2)}\right]=\int_{-b/2}^{+b/2}\int_{z_{k_j}-h_{k_j}/2}^{z_{k_j}+h_{k_j}/2}\left[1,(z-z_k),(z-z_k)^2\right]dz\,dy \tag{30}$$

$$\left[I_{ek_j}^{(1)}, I_{ek_j}^{(2)}, I_{ek_j}^{(3)}, I_{mek_j}\right] = \int_{-b/2}^{+b/2}\int_{z_{k_j}-h_{k_j}/2}^{z_{k_j}+h_{k_j}/2}\left[(z-z_{k_j}),(z-z_{k_j})^2,(z-z_{k_j})^3,(z-z_k)(z-z_{k_j})\right]dz\,dy$$

$$\left[A_{cs}, I_{cs}^{(1)}, I_{cs}^{(2)}, I_{cs}^{(3)}\right] = \int_{-b/2}^{+b/2}\int_{-h_{cs}/2}^{+h_{cs}/2}\left[1, z^2, z^4, z^6\right]dz\,dy$$

$$\left[A_{ce}, I_{ce}^{(1)}, I_{ce}^{(2)}, I_{ce}^{(3)}\right] = \int_{-b/2}^{+b/2}\int_{-h_{ce}-h_{cs}/2}^{-h_{cs}/2}\left[1, z^2, z^4, z^6\right]dz\,dy + \int_{-b/2}^{+b/2}\int_{+h_{cs}/2}^{+h_{ce}+h_{cs}/2}\left[1, z^2, z^4, z^6\right]dz\,dy$$

with

$$z_{k_j} = \pm\frac{h_{k_j}+h_c}{2} \pm \sum_{r=1}^{j-1} h_{k_r}; \quad k = a(+), b(-) \tag{31}$$

The kinetic energy of the multilayer beam is,

$$T = T_{cs} + T_{ce} + \sum_{k=a}^{b}\sum_{j=1}^{n,m} T_{k_j} \tag{32}$$

where

$$\begin{aligned} T_{k_j} &= \frac{1}{2}\int_{V_{k_j}} \rho_{k_j}\left(\dot{u}_k^2 + \dot{w}^2\right)dv_{k_j} \\ T_{cs} &= \frac{1}{2}\int_{V_{cs}} \rho_{cs}\left(\dot{u}_c^2 + \dot{w}^2\right)dv_{cs} \\ T_{ce} &= \frac{1}{2}\int_{V_{ce}} \rho_{ce}\left(\dot{u}_c^2 + \dot{w}^2\right)dv_{ce} \end{aligned} \tag{33}$$

and ρ_l is the density of each layer ($l = k_j, cs, ce$). Applying the variational operator, integrating by parts, using the displacement fields (Eq. (2)) and integrating through the thickness yields the following relations:

$$\delta T_{k_j} = -\int_0^L \rho_{k_j}\left[A_{k_j}\left(\delta u_k \ddot{u}_k + \delta w \ddot{w}\right) - I_{mk_j}^{(1)}\left(\delta u_k \ddot{w}' + \delta w' \ddot{u}_k\right) + I_{mk_j}^{(2)}\delta w' \ddot{w}'\right]dx \tag{34}$$

$$\delta T_{cs} = -\int_0^L \rho_{cs}\left\{\begin{array}{l} A_{cs}\left(\delta u_c \ddot{u}_c + \delta w \ddot{w}\right) \\ +I_{cs}^{(1)}\delta\beta_c\,\ddot{\beta}_c \\ -\dfrac{4I_{cs}^{(2)}}{3h_c^2}\left[\delta\beta_c\left(\ddot{\beta}_c + \ddot{w}'\right) + \left(\delta\beta_c + \delta w'\right)\ddot{\beta}_c\right] \\ +\dfrac{16I_{cs}^{(3)}}{9h_c^4}\left(\delta\beta_c + \delta w'\right)\left(\ddot{\beta}_c + \ddot{w}'\right) \end{array}\right\}dx \tag{35}$$

$$\delta T_{ce} = -\int_0^L \rho_{ce} \begin{Bmatrix} A_{ce}\left(\delta u_c \ddot{u}_c + \delta w \ddot{w}\right) \\ +I_{ce}^{(1)} \delta\beta_c \ddot{\beta}_c \\ -\frac{4I_{ce}^{(2)}}{3h_c^2}\left[\delta\beta_c\left(\ddot{\beta}_c + \ddot{w}'\right) + \left(\delta\beta_c + \delta w'\right)\ddot{\beta}_c\right] \\ +\frac{16I_{ce}^{(3)}}{9h_c^4}\left(\delta\beta_c + \delta w'\right)\left(\ddot{\beta}_c + \ddot{w}'\right) \end{Bmatrix} dx \tag{36}$$

Moreover, the virtual works of applied conservative forces are the same as presented in [9].

In case of clamped-free mechanical boundary condition, the non-conservative work must be taken into account,

$$\delta W_k^{NC} = \sum_{j=1}^{n,m} \delta W_{k_j}^{NC} \tag{37}$$

with

$$\delta W_{k_j}^{NC} = -P_{k_j} \varepsilon_t\left(L\right) \delta w\left(L\right) \tag{38}$$

where P_{k_j} is the piezoelectric force in the j -th extension piezoelectric layer due to considering the von Karman's displacement-strain relation and it can be expressed as follows:

$$P_{k_j} = -e_{31}^{k_j^*} A_{k_j} \frac{V_{k_j}}{h_{k_j}} \tag{39}$$

Since in the case of pinned-pinned, clamped-clamped or clamped-pinned mechanical boundary conditions, $\delta w\left(L\right) = 0$, there is no need to take account of Eq. (37) in calculation of Eq. (24) for the mentioned mechanical boundary conditions.

3. Dynamic finite element model

In this section, a finite element model for the multilayer beam is developed based on the expressions of the virtual works in the variational formulation. Lagrangian shape functions are considered for the longitudinal displacement of the core layers u_c . For transverse displacement, w , Hermite cubic shape functions are assumed. The V_{k_j} of the face piezoelectric layers and V_c of the core piezoelectric layer are assumed to be constant within an element. A quadratic shape function is used for the section rotation β_c in order to avoid shear locking and also for the coefficient ψ_3 to satisfy the electrostatic equilibrium condition [9]. Hence, the elemental DoF column vector $\hat{\mathbf{q}}$ is defined as:

$$\hat{\mathbf{q}} = \begin{pmatrix} u_c^{(1)}, w^{(1)}, w'^{(1)}, \beta_c^{(1)}, u_c^{(2)}, w^{(2)}, w'^{(2)}, \beta_c^{(2)}, \psi_3^{(1)}, \psi_3^{(2)} \\ , \beta_c^{(0)}, \psi_3^{(0)}, V_{a1}^{(0)}, ..., V_{a\ell}^{(0)}, V_{b1}^{(0)}, ..., V_{bp}^{(0)}, V_{c_s}^{(0)} \\ , V_{al+1}^{(0)}, ..., V_{ax}^{(0)}, V_{bp+1}^{(0)}, ..., V_{by}^{(0)}, V_{c_a}^{(0)} \end{pmatrix}^T \tag{40}$$

where $\wedge$ is used to define the elemental quantities. $V_{a1}^{(0)},...,V_{a\ell}^{(0)},V_{b1}^{(0)},...,V_{bp}^{(0)},V_{c_s}^{(0)}$ correspond to piezoelectric layers acting as sensors and $V_{al+1}^{(0)},...,V_{ax}^{(0)},V_{bp+1}^{(0)},...,V_{by}^{(0)},V_{c_a}^{(0)}$ correspond to piezoelectric layers acting as actuators. Figure 2 shows the element with its degrees of freedom.

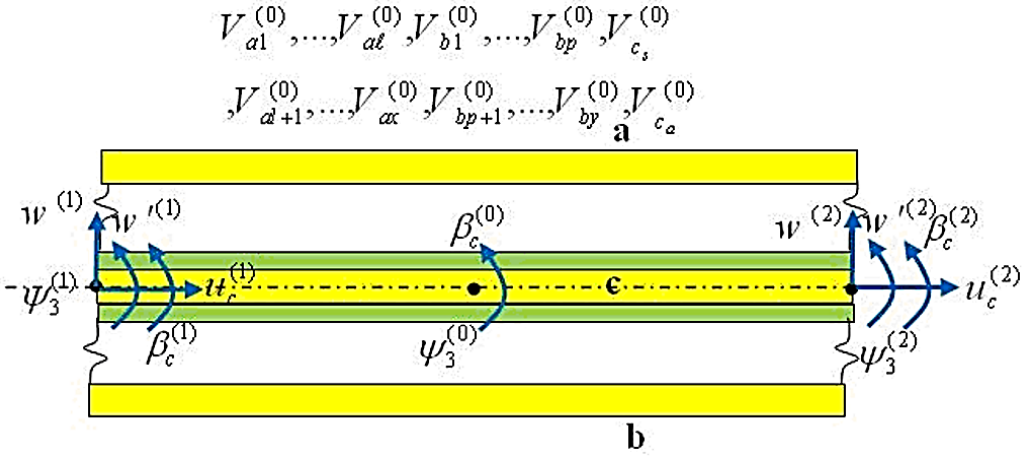

Fig. 2. The finite element degrees of freedom for the multilayer beam element

In spite of defining $V_{a1}^{(0)},...,V_{a\ell}^{(0)},V_{b1}^{(0)},...,V_{bp}^{(0)},V_{c_s}^{(0)}$ for an element, another important condition should be met for sensor voltages of piezoelectric layers. Each piezoelectric layer, acting as a sensor, should have only one sensor voltage. This voltage must be equal to the rest of voltages of the elements representing that specific piezoelectric layer, i.e. $V_{a1}^{(0)}$ for element number 1 should be equal to $V_{a1}^{(0)}$ for element number 2 and other elements which are representing one specific piezoelectric layer. In the following section, it is explained how to apply such condition.

By applying Eq. (40) to Eqs. (27), (28) and (29), the discretized virtual works of the elemental electromechanical internal forces of the face piezoelectric layers $\delta\hat{H}_{k_j}$, the piezoelectric core layers $\delta\hat{H}_{cs}$ and the elastic core layers $\delta\hat{H}_{ce}$ are given as follows:

$$\begin{aligned} \delta\hat{H}_{k_j} &= \delta\hat{\mathbf{q}}^T \left(\hat{\mathbf{K}}_{k_j m} - \hat{\mathbf{K}}_{k_j me} + \hat{\mathbf{K}}_{k_j e} + \hat{\mathbf{K}}_{k_j me_N} \right) \hat{\mathbf{q}} = \delta\hat{\mathbf{q}}^T \hat{\mathbf{K}}_{k_j} \hat{\mathbf{q}} \\ \delta\hat{H}_{cs} &= \delta\hat{\mathbf{q}}^T \left(\hat{\mathbf{K}}_{csm} - \hat{\mathbf{K}}_{csme} + \hat{\mathbf{K}}_{cse} \right) \hat{\mathbf{q}} = \delta\hat{\mathbf{q}}^T \hat{\mathbf{K}}_{cs} \hat{\mathbf{q}} \\ \delta\hat{H}_{ce} &= \delta\hat{\mathbf{q}}^T \left(\hat{\mathbf{K}}_{cem} \right) \hat{\mathbf{q}} \end{aligned} \tag{41}$$

where the elemental mechanical $\hat{\mathbf{K}}_{k_j m}$, piezoelectric $\hat{\mathbf{K}}_{k_j me}$, dielectric $\hat{\mathbf{K}}_{k_j e}$ and nonlinear piezoelectric $\hat{\mathbf{K}}_{k_j me_N}$ stiffness matrices of the k_j -th face layers are:

$$\hat{\mathbf{K}}_{k_j m} = \int_0^{L_e} \left\{ \begin{array}{l} c_{11}^{k_j^*} \left[A_{k_j} \mathbf{B}_{km}^T \mathbf{B}_{km} + I_{mk_j}^{(1)} \left(\mathbf{B}_{km}^T \mathbf{B}_{kb} + \mathbf{B}_{kb}^T \mathbf{B}_{km} \right) + I_{mk_j}^{(2)} \mathbf{B}_{kb}^T \mathbf{B}_{kb} \right] \\ + \dfrac{e_{31}^{k_j^* 2}}{\in_{33}^{k_j^*}} \left(I_{ek_j}^{(1)} \mathbf{B}_{km}^T \mathbf{B}_{kb} + 2 I_{mek_j} \mathbf{B}_{kb}^T \mathbf{B}_{kb} + I_{ek_j}^{(1)} \mathbf{B}_{kb}^T \mathbf{B}_{km} - I_{ek_j}^{(2)} \mathbf{B}_{kb}^T \mathbf{B}_{kb} \right) \\ - \dfrac{\in_{11}^{k_j} e_{31}^{k_j^* 2}}{4 \in_{33}^{k_j^* 2}} \left(I_{ek_j}^{(3)} + \dfrac{A_{k_j} h_{k_j}^4}{16} - \dfrac{I_{ek_j}^{(2)} h_{k_j}^2}{2} \right) \mathbf{B}_{kb}^{\prime T} \mathbf{B}_{kb}^{\prime} \end{array} \right\} dx$$

$$\hat{\mathbf{K}}_{k_j me} = -\int_0^{L_e} \left\{ \frac{e_{31}^{k_j^*}}{h_{k_j}} \left[\begin{array}{l} A_{k_j} \left(\mathbf{B}_{km}^T \mathbf{N}_{Pk_j} + \mathbf{N}_{Pk_j}^T \mathbf{B}_{km} \right) + I_{mk_j}^{(1)} \left(\mathbf{B}_{kb}^T \mathbf{N}_{Pk_j} + \mathbf{N}_{Pk_j}^T \mathbf{B}_{kb} \right) \\ - I_{ek_j}^{(1)} \left(\mathbf{B}_{kb}^T \mathbf{N}_{Pk_j} + \mathbf{N}_{Pk_j}^T \mathbf{B}_{kb} \right) \end{array} \right] \right\} dx \tag{42}$$

$$\hat{\mathbf{K}}_{k_j e} = -\int_0^{L_e} \left\{ \in_{33}^{k_j^*} \frac{A_{k_j}}{h_{k_j}^2} \mathbf{N}_{Pk_j}^T \mathbf{N}_{Pk_j} \right\} dx$$

$$\hat{\mathbf{K}}_{k_j me_N} = \int_0^{L_e} \left\{ e_{31}^{k_j^*} \frac{A_{k_j}}{h_{k_j}} \mathbf{B}_t^T \mathbf{B}_t \left(\mathbf{N}_{Pk_j} \right) \right\} dx$$

L_e is the element length. $\mathbf{B}_{km}$, $\mathbf{B}_{kb}$ and $\mathbf{B}_t$ are the membrane, bending strain and section rotation operators of the face layers. $\mathbf{N}_{Pk_j}$ is the interpolation matrix used for V_{k_j} in the face layers.

In the matrix $\hat{\mathbf{K}}_{k_j m}$, the presence of the terms

$\dfrac{e_{31}^{k_j^* 2}}{\in_{33}^{k_j^*}} \left(I_{ek_j}^{(1)} \mathbf{B}_{km}^T \mathbf{B}_{kb} + 2 I_{mek_j} \mathbf{B}_{kb}^T \mathbf{B}_{kb} + I_{ek_j}^{(1)} \mathbf{B}_{kb}^T \mathbf{B}_{km} - I_{ek_j}^{(2)} \mathbf{B}_{kb}^T \mathbf{B}_{kb} \right)$ and

$-\dfrac{\in_{11}^{k_j} e_{31}^{k_j^* 2}}{4 \in_{33}^{k_j^* 2}} \left(I_{ek_j}^{(3)} + \dfrac{A_{k_j} h_{k_j}^4}{16} - \dfrac{I_{ek_j}^{(2)} h_{k_j}^2}{2} \right) \mathbf{B}_{kb}^{\prime T} \mathbf{B}_{kb}^{\prime}$ are due to considering higher-order terms for the longitudinal and transverse electric fields, respectively. In addition, the presence of the matrix $\hat{\mathbf{K}}_{k_j me_N}$ is due to considering the von Karman's displacement-strain. This new electromechanical matrix is valid for both the extension piezoelectric sensor and actuator.

The elemental stiffness matrices of the core layers, $\hat{\mathbf{K}}_{csm}$, $\hat{\mathbf{K}}_{csme}$ and $\hat{\mathbf{K}}_{cse}$ are expressed as follows:

$$\hat{\mathbf{K}}_{csm} = \int_0^{L_e} \left\{ \begin{array}{l} c_{33}^{c^*} \left[\begin{array}{l} A_{cs}\mathbf{B}_{cm}^T\mathbf{B}_{cm} + I_{cs}^{(1)}\mathbf{B}_{cb}^T\mathbf{B}_{cb} - \dfrac{4I_{cs}^{(2)}}{3h_c^2}\left(\mathbf{B}_{cb}^T\mathbf{B}_{ch} + \mathbf{B}_{ch}^T\mathbf{B}_{cb}\right) \\ + \dfrac{16I_{cs}^{(3)}}{9h_c^4}\mathbf{B}_{ch}^T\mathbf{B}_{ch} \end{array} \right] \\ + c_{55}^{c}\left(A_{cs} + \dfrac{16I_{cs}^{(2)}}{h_c^4} - \dfrac{8I_{cs}^{(1)}}{h_c^2}\right)\mathbf{B}_{cs}^T\mathbf{B}_{cs} \end{array} \right\} dx$$

$$\hat{\mathbf{K}}_{csme} = -\int_0^{L_e} \left\{ \begin{array}{l} \dfrac{e_{33}^{c^*}}{h_{cs}}\left(\dfrac{I_{cs}^{(2)}}{h_{cs}^2} - \dfrac{I_{cs}^{(1)}}{4}\right)\left(\mathbf{B}_{cb}^T\mathbf{N}'_{\psi_3} + \mathbf{N}'^T_{\psi_3}\mathbf{B}_{cb}\right) \\ - \dfrac{4e_{33}^{c^*}}{3h_c^2h_{cs}}\left(\dfrac{I_{cs}^{(3)}}{h_{cs}^2} - \dfrac{I_{cs}^{(2)}}{4}\right)\left(\mathbf{B}_{ch}^T\mathbf{N}'_{\psi_3} + \mathbf{N}'^T_{\psi_3}\mathbf{B}_{ch}\right) \\ + \dfrac{e_{15}^{c}}{2h_{cs}}\left(A_{cs} - \dfrac{4I_{cs}^{(1)}}{h_c^2}\right)\left(\mathbf{B}_{cs}^T\mathbf{N}_{V_c} + \mathbf{N}_{V_c}^T\mathbf{B}_{cs}\right) \\ + \dfrac{e_{15}^{c}}{2h_{cs}}\left(\dfrac{3I_{cs}^{(1)}}{h_{cs}^2} + \dfrac{I_{cs}^{(1)}}{h_c^2} - \dfrac{12I_{cs}^{(2)}}{h_{cs}^2h_c^2} - \dfrac{A_{cs}}{4}\right)\left(\mathbf{B}_{cs}^T\mathbf{N}_{\psi_3} + \mathbf{N}_{\psi_3}^T\mathbf{B}_{cs}\right) \end{array} \right\} dx \quad (43)$$

$$\hat{\mathbf{K}}_{cse} = -\int_0^{L_e} \left\{ \begin{array}{l} \in_{33}^{c^*}\left(\dfrac{I_{cs}^{(3)}}{h_{cs}^6} + \dfrac{I_{cs}^{(1)}}{16h_{cs}^2} - \dfrac{I_{cs}^{(2)}}{2h_{cs}^4}\right)\mathbf{N}'^T_{\psi_3}\mathbf{N}'_{\psi_3} + \dfrac{\in_{11}^{c}A_{cs}}{h_{cs}^2}\mathbf{N}_{V_c}^T\mathbf{N}_{V_c} \\ + \dfrac{\in_{11}^{c}}{h_{cs}^2}\left(\dfrac{3I_{cs}^{(1)}}{h_{cs}^2} - \dfrac{A_{cs}}{4}\right)\left(\mathbf{N}_{V_c}^T\mathbf{N}_{\psi_3} + \mathbf{N}_{\psi_3}^T\mathbf{N}_{V_c}\right) \\ + \dfrac{\in_{11}^{c}}{h_{cs}^2}\left(\dfrac{9I_{cs}^{(2)}}{h_{cs}^4} + \dfrac{A_{cs}}{16} - \dfrac{3I_{cs}^{(1)}}{2h_{cs}^2}\right)\mathbf{N}_{\psi_3}^T\mathbf{N}_{\psi_3} \end{array} \right\} dx$$

The matrix $\hat{\mathbf{K}}_{cem}$ for the elastic core layer is:

$$\hat{\mathbf{K}}_{cem} = \int_0^{L_e} \left\{ \begin{array}{l} c_{11}^{ce} \left[\begin{array}{l} A_{ce}\mathbf{B}_{cm}^T\mathbf{B}_{cm} + I_{ce}^{(1)}\mathbf{B}_{cb}^T\mathbf{B}_{cb} - \dfrac{4I_{ce}^{(2)}}{3h_c^2}\left(\mathbf{B}_{cb}^T\mathbf{B}_{ch} + \mathbf{B}_{ch}^T\mathbf{B}_{cb}\right) \\ + \dfrac{16I_{ce}^{(3)}}{9h_c^4}\mathbf{B}_{ch}^T\mathbf{B}_{ch} \end{array} \right] \\ + c_{55}^{ce}\left(A_{ce} + \dfrac{16I_{ce}^{(2)}}{h_c^4} - \dfrac{8I_{ce}^{(1)}}{h_c^2}\right)\mathbf{B}_{cs}^T\mathbf{B}_{cs} \end{array} \right\} dx \quad (44)$$

Similarly, by using the elemental DoF vector (Eq. (40)), the discretized virtual works of the inertial forces $\delta\hat{T}_{p_j}$, $\delta\hat{T}_{cs}$ and $\delta\hat{T}_{ce}$ are written as,

$$\begin{aligned} \delta\hat{T}_{k_j} &= -\delta\hat{\mathbf{q}}^T\left(\hat{\mathbf{M}}_{k_jt} - \hat{\mathbf{M}}_{k_jtr}^T - \hat{\mathbf{M}}_{k_jtr} + \hat{\mathbf{M}}_{k_jr}\right)\ddot{\hat{\mathbf{q}}} = -\delta\hat{\mathbf{q}}^T\hat{\mathbf{M}}_{k_j}\ddot{\hat{\mathbf{q}}} \\ \delta\hat{T}_{cs} &= -\delta\hat{\mathbf{q}}^T\left(\hat{\mathbf{M}}_{cst} - \hat{\mathbf{M}}_{csrs}^T - \hat{\mathbf{M}}_{csrs} + \hat{\mathbf{M}}_{csr} + \hat{\mathbf{M}}_{css}\right)\ddot{\hat{\mathbf{q}}} = -\delta\hat{\mathbf{q}}^T\hat{\mathbf{M}}_{cs}\ddot{\hat{\mathbf{q}}} \\ \delta\hat{T}_{ce} &= -\delta\hat{\mathbf{q}}^T\left(\hat{\mathbf{M}}_{cet} - \hat{\mathbf{M}}_{cers}^T - \hat{\mathbf{M}}_{cers} + \hat{\mathbf{M}}_{cer} + \hat{\mathbf{M}}_{ces}\right)\ddot{\hat{\mathbf{q}}} = -\delta\hat{\mathbf{q}}^T\hat{\mathbf{M}}_{ce}\ddot{\hat{\mathbf{q}}} \end{aligned} \quad (45)$$

where $\ddot{\hat{\mathbf{q}}}$ is the elemental acceleration vector. The elemental mass matrices of the multilayer beam can be expressed as follows:

$$
\begin{aligned}
\hat{\mathbf{M}}_{k_j t} &= \int_0^{L_e} \rho_{k_j} A_{k_j} \left(\mathbf{N}_{kx}^T \mathbf{N}_{kx} + \mathbf{N}_z^T \mathbf{N}_z \right) dx \\
\hat{\mathbf{M}}_{k_j tr} &= \int_0^{L_e} \rho_{k_j} I_{mk_j}^{(1)} \mathbf{N}_{kx}^T \mathbf{N}_{kr}\, dx \\
\hat{\mathbf{M}}_{k_j r} &= \int_0^{L_e} \rho_{k_j} I_{mk_j}^{(2)} \mathbf{N}_{kr}^T \mathbf{N}_{kr}\, dx \\
\hat{\mathbf{M}}_{cst} &= \int_0^{L_e} \rho_{cs} A_{cs} \left(\mathbf{N}_{cx}^T \mathbf{N}_{cx} + \mathbf{N}_z^T \mathbf{N}_z \right) dx \\
\hat{\mathbf{M}}_{csr} &= \int_0^{L_e} \rho_{cs} I_{cs}^{(1)} \mathbf{N}_{cr}^T \mathbf{N}_{cr}\, dx \\
\hat{\mathbf{M}}_{csrs} &= \int_0^{L_e} \rho_{cs} \frac{4 I_{cs}^{(2)}}{3 h_c^2} \mathbf{N}_{cr}^T \mathbf{N}_{cs}\, dx \\
\hat{\mathbf{M}}_{css} &= \int_0^{L_e} \rho_{cs} \frac{16 I_{cs}^{(3)}}{9 h_c^4} \mathbf{N}_{cs}^T \mathbf{N}_{cs}\, dx \\
\hat{\mathbf{M}}_{cet} &= \int_0^{L_e} \rho_{ce} A_{ce} \left(\mathbf{N}_{cx}^T \mathbf{N}_{cx} + \mathbf{N}_z^T \mathbf{N}_z \right) dx \\
\hat{\mathbf{M}}_{cer} &= \int_0^{L_e} \rho_{ce} I_{ce}^{(1)} \mathbf{N}_{cr}^T \mathbf{N}_{cr}\, dx \\
\hat{\mathbf{M}}_{cers} &= \int_0^{L_e} \rho_{ce} \frac{4 I_{ce}^{(2)}}{3 h_c^2} \mathbf{N}_{cr}^T \mathbf{N}_{cs}\, dx \\
\hat{\mathbf{M}}_{ces} &= \int_0^{L_e} \rho_{ce} \frac{16 I_{ce}^{(3)}}{9 h_c^4} \mathbf{N}_{cs}^T \mathbf{N}_{cs}\, dx
\end{aligned}
\tag{46}
$$

where $\mathbf{N}_{ix}$, $\mathbf{N}_z$, $\mathbf{N}_{ir}$ and $\mathbf{N}_{cs}$ are the translations in *x* and *z* directions, rotation and shear interpolation matrices. A Lagrange linear interpolation is assumed for β_c to evaluate the corresponding mass matrices since it is highly recommended to perform a static condensation of the elemental core section rotation $\beta_c^{(0)}$ [13].

The discretized virtual work of the conservative forces is:

$$
\delta \hat{W}^C = \delta \hat{\mathbf{q}}^T \hat{\mathbf{F}}_m \tag{47}
$$

where the generalized forces are:

$$
\hat{\mathbf{F}}_m = \int_0^{L_e} \begin{bmatrix} \mathbf{N}_{ax}^T n_a + \mathbf{N}_{bx}^T n_b + \mathbf{N}_{cx}^T n_c + \mathbf{N}_z^T \left(q_a + q_b + q_c \right) \\ -\mathbf{N}_{ar}^T \left(m_a + m_b \right) + \mathbf{N}_{cr}^T m_c - \mathbf{N}_{cs}^T p_c \end{bmatrix} dx \tag{48}
$$

Moreover, to compute the distributed load vectors, a linear interpolation for β_c is used to avoid any induced equivalent nodal load contributions for $\beta_c^{(0)}$. Therefore, the static condensation of this degree of freedom will be easier [13].

The discretized virtual work of the non-conservative force is:

$$\delta \hat{W}_{k_j}^{NC} = \delta \hat{\mathbf{q}}^T \hat{\mathbf{K}}_{k_j NC} \delta \hat{\mathbf{q}} = \delta \hat{\mathbf{q}}^T \left(P_{k_j} \mathbf{B}_t^T \Big|_{x=L} \mathbf{B}_t \Big|_{x=L} \right) \delta \hat{\mathbf{q}} \tag{49}$$

Apparently, the discretized virtual work of the non-conservative force can be added to the stiffness matrix of the element. Hence, the discretized variational formulation for an element is written as follows:

$$\left(\hat{\mathbf{M}}_f + \hat{\mathbf{M}}_c \right) \ddot{\hat{\mathbf{q}}} + \left(\hat{\mathbf{K}}_f + \hat{\mathbf{K}}_c + \hat{\mathbf{K}}_{NC} \right) \hat{\mathbf{q}} = \hat{\mathbf{F}}_m \tag{50}$$

where $\hat{\mathbf{M}}_f = \sum_k \sum_j \hat{\mathbf{M}}_{k_j}$, $\hat{\mathbf{K}}_f = \sum_k \sum_j \hat{\mathbf{K}}_{k_j}$ and $\hat{\mathbf{K}}_{NC} = \sum_k \sum_j \hat{\mathbf{K}}_{k_j NC}$. Since there are no inertial electric DoFs, the mechanical and electric DoFs are coupled statically. Thus, in pursuit of a faster and more reliable solution and also, to prevent the ill-conditioning problem, the static condensation is performed to eliminate the electric DoFs. Since there are elemental ($V_{a_j}^{(0)}$,$V_{b_j}^{(0)}$, $V_c^{(0)}$ and $\psi_3^{(0)}$) and nodal ($\psi_3^{(1)}$ and $\psi_3^{(2)}$) electric DoFs, the static condensation is performed in two steps: First, the unknown elemental DoFs are condensed at the element level; second, after assembling, the nodal electric DoFs are condensed at the global level [13]. Since the von Karman's displacement-strain relation is used here, the obtained finite element model is a nonlinear model. Therefore, before global condensing, the governing equations are linearized.

3.1. Static condensation

In this section, in order to apply the static condensation, the elemental DoFs vector is decomposed. When there is an actuator, an elemental DoFs vector $\hat{\mathbf{q}}_a$ corresponding to the ($V_{a_j}^{(0)}$, $V_{b_j}^{(0)}$ and $V_c^{(0)}$) is defined. For the sensor case of face and core piezoelectric layers, unknown elemental DoFs vectors $\hat{\mathbf{q}}_{s_k}$ and $\hat{\mathbf{q}}_{s_c}$ corresponding to ($V_{a_j}^{(0)}$ and $V_{b_j}^{(0)}$) and ($V_c^{(0)}$) respectively are not defined. Even for the actuator case, when $V_c^{(0)}$ is prescribed, the variables ($\psi_3^{(0)}$, $\psi_3^{(1)}$ and $\psi_3^{(2)}$) are still unknown. Since the nodal electric DoFs $\psi_3^{(1)}$ and $\psi_3^{(2)}$ are to be condensed after assembling, a DoFs vector $\hat{\mathbf{q}}_e$ is introduced. In addition, both elemental variables $\psi_3^{(0)}$ and $\beta_c^{(0)}$ are defined by a DoFs vector $\hat{\mathbf{q}}_c$. Therefore, the elemental DoF vector is decomposed as follows:

$$\hat{\mathbf{q}} = \left(\hat{\mathbf{q}}_m, \hat{\mathbf{q}}_e, \hat{\mathbf{q}}_c, \hat{\mathbf{q}}_{s_k}, \hat{\mathbf{q}}_{s_c}, \hat{\mathbf{q}}_a \right)^T \tag{51}$$

where

$$\begin{aligned} \hat{\mathbf{q}}_m &= \left(u_c^{(1)}, w^{(1)}, w'^{(1)}, \beta_c^{(1)}, u_c^{(2)}, w^{(2)}, w'^{(2)}, \beta_c^{(2)} \right)^T \\ \hat{\mathbf{q}}_e &= \left(\psi_3^{(1)}, \psi_3^{(2)} \right)^T \\ \hat{\mathbf{q}}_c &= \left(\beta_c^{(0)}, \psi_3^{(0)} \right)^T \end{aligned} \tag{52}$$

$$\hat{\mathbf{q}}_{s_k} = \left(V_{a1}^{(0)},...,V_{a\ell}^{(0)},V_{b1}^{(0)},...,V_{bp}^{(0)}\right)^T$$

$$\hat{\mathbf{q}}_{s_c} = \left(V_{cs}^{(0)}\right)^T$$

$$\hat{\mathbf{q}}_a = \left(V_{al+1}^{(0)},...,V_{ax}^{(0)},V_{bp+1}^{(0)},...,V_{by}^{(0)},V_{ca}^{(0)}\right)^T$$

According to the aforementioned definitions, the matrices $\hat{\mathbf{K}}_{k_j me_N}$ and $\hat{\mathbf{K}}_{k_j NC}$ for sensor and actuator cases are rewritten as:

$$\begin{aligned}\hat{\mathbf{K}}_{k_j me_N} &= \int_0^{L_e}\left\{e_{31}^{k_j^*}\frac{A_{k_j}}{h_{k_j}}\mathbf{B}_t^T\mathbf{B}_t\left[V_{k_j s}\ or\ V_{k_j a}\right]\right\}dx = \int_0^{L_e}\left\{e_{31}^{k_j^*}\frac{A_{k_j}}{h_{k_j}}\mathbf{B}_t^T\mathbf{B}_t\left[\mathbf{N}_{P^*k_j}\mathbf{q}_{s_k}\ or\ \mathbf{N}_{P^*k_j}\mathbf{q}_a\right]\right\}dx \\ \hat{\mathbf{K}}_{k_j NC} &= -e_{31}^{k_j^*}\frac{A_{k_j}}{h_{k_j}}\mathbf{B}_t^T\Big|_{x=L}\mathbf{B}_t\Big|_{x=L}\left(V_{k_j s}\ or\ V_{k_j a}\right) = -e_{31}^{k_j^*}\frac{A_{k_j}}{h_{k_j}}\mathbf{B}_t^T\Big|_{x=L}\mathbf{B}_t\Big|_{x=L}\left(\mathbf{N}_{P^*k_j}\mathbf{q}_{s_k}\ or\ \mathbf{N}_{P^*k_j}\mathbf{q}_a\right)\end{aligned} \tag{53}$$

where $V_{k_j s}$ and $V_{k_j a}$ are the voltages corresponding to each face piezoelectric sensor and actuator respectively. $\mathbf{q}_{s_k}$ and $\mathbf{q}_a$ are the electric sensing and actuating voltage vectors of each face piezoelectric sensor and actuator respectively. $\mathbf{N}_{P^*k_j}$ is defined as:

$$\begin{bmatrix}\mathbf{N}_{P^*a_1}\\ \vdots\\ \mathbf{N}_{P^*b_p}\\ \mathbf{N}_{P^*a_{l+1}}\\ \vdots\\ \mathbf{N}_{P^*b_y}\end{bmatrix} = \begin{bmatrix}1 & & 0 & 0 & & 0\\ & \ddots & & & \ddots & \vdots\\ 0 & & 1 & 0 & & 0\\ 0 & & 0 & 1 & & 0\\ & \ddots & & & \ddots & \vdots\\ 0 & & 0 & 0 & & 1\end{bmatrix} \tag{54}$$

Hence, Eq. (50) can be decomposed as:

$$\begin{bmatrix}\hat{\mathbf{M}} & \cdots & \mathbf{0}\\ \vdots & \ddots & \vdots\\ \mathbf{0} & \cdots & \mathbf{0}\end{bmatrix}\begin{Bmatrix}\ddot{\hat{\mathbf{q}}}_m\\ \ddot{\hat{\mathbf{q}}}_e\\ \ddot{\hat{\mathbf{q}}}_c\\ \ddot{\hat{\mathbf{q}}}_{s_k}\\ \ddot{\hat{\mathbf{q}}}_{s_c}\\ \ddot{\hat{\mathbf{q}}}_a\end{Bmatrix} + \begin{bmatrix}\hat{\mathbf{K}}_{mm}\left(\mathbf{q}_{s_k},\mathbf{q}_a\right) & -\hat{\mathbf{K}}_{me} & -\hat{\mathbf{K}}_{mc} & -\hat{\mathbf{K}}_{ms_k} & -\hat{\mathbf{K}}_{ms_c} & -\hat{\mathbf{K}}_{ma}\\ & \hat{\mathbf{K}}_{ee} & -\hat{\mathbf{K}}_{ec} & \mathbf{0} & -\hat{\mathbf{K}}_{es_c} & -\hat{\mathbf{K}}_{ea}\\ & & \hat{\mathbf{K}}_{cc} & -\hat{\mathbf{K}}_{cs_k} & -\hat{\mathbf{K}}_{cs_c} & -\hat{\mathbf{K}}_{ca}\\ & & & \hat{\mathbf{K}}_{s_k s_k} & \mathbf{0} & \mathbf{0}\\ & sym & & & \hat{\mathbf{K}}_{s_c s_c} & \mathbf{0}\\ & & & & & \hat{\mathbf{K}}_{aa}\end{bmatrix}\begin{Bmatrix}\hat{\mathbf{q}}_m\\ \hat{\mathbf{q}}_e\\ \hat{\mathbf{q}}_c\\ \hat{\mathbf{q}}_{s_k}\\ \hat{\mathbf{q}}_{s_c}\\ \hat{\mathbf{q}}_a\end{Bmatrix} = \begin{Bmatrix}\hat{\mathbf{F}}_m\\ \mathbf{0}\\ \mathbf{0}\\ \mathbf{0}\\ \mathbf{0}\\ \mathbf{0}\end{Bmatrix} \tag{55}$$

Since $\hat{\mathbf{q}}_a$ is defined, its virtual variation $\delta\hat{\mathbf{q}}_a$ vanishes. Hence, the sixth line of Eq. (55) is automatically satisfied and can be neglected. In addition, the remaining terms corresponding to $\hat{\mathbf{q}}_a$ have to be moved to the right hand side leading to the following equivalent electric load vectors:

$$\begin{aligned}\hat{\mathbf{F}}_{ma} &= \hat{\mathbf{K}}_{ma}\hat{\mathbf{q}}_a \\ \hat{\mathbf{F}}_{ca} &= \hat{\mathbf{K}}_{ca}\hat{\mathbf{q}}_a \\ \hat{\mathbf{F}}_{ea} &= \hat{\mathbf{K}}_{ea}\hat{\mathbf{q}}_a\end{aligned} \tag{56}$$

Considering the non-singularity of matrix $\hat{\mathbf{K}}_{cc}$, the third line of Eq. (55) can be solved for $\hat{\mathbf{q}}_c$ as follows:

$$\hat{\mathbf{q}}_c = \hat{\mathbf{K}}_{cc}^{-1}\left(\hat{\mathbf{K}}_{cm}\hat{\mathbf{q}}_m + \hat{\mathbf{K}}_{ce}\hat{\mathbf{q}}_e + \hat{\mathbf{K}}_{cs_k}\hat{\mathbf{q}}_{s_k} + \hat{\mathbf{K}}_{cs_c}\hat{\mathbf{q}}_{s_c} + \hat{\mathbf{F}}_{ca}\right) \tag{57}$$

Replacing Eqs. (56) and (57) in Eq. (55) yields the following equation:

$$\begin{bmatrix}\hat{\mathbf{M}} & \cdots & \mathbf{0} \\ \vdots & \ddots & \vdots \\ \mathbf{0} & \cdots & \mathbf{0}\end{bmatrix}\begin{Bmatrix}\ddot{\hat{\mathbf{q}}}_m \\ \ddot{\hat{\mathbf{q}}}_e \\ \ddot{\hat{\mathbf{q}}}_{s_k} \\ \ddot{\hat{\mathbf{q}}}_{s_c}\end{Bmatrix} + \begin{bmatrix}\hat{\mathbf{K}}^*_{mm}\left(\mathbf{q}_{s_k},\mathbf{q}_a\right) & -\hat{\mathbf{K}}^*_{me} & -\hat{\mathbf{K}}^*_{ms_k} & -\hat{\mathbf{K}}^*_{ms_c} \\ & \hat{\mathbf{K}}^*_{ee} & -\hat{\mathbf{K}}^*_{es_k} & -\hat{\mathbf{K}}^*_{es_c} \\ & & \hat{\mathbf{K}}^*_{s_ks_k} & -\hat{\mathbf{K}}^*_{s_ks_c} \\ & sym & & \hat{\mathbf{K}}^*_{s_cs_c}\end{bmatrix}\begin{Bmatrix}\hat{\mathbf{q}}_m \\ \hat{\mathbf{q}}_e \\ \hat{\mathbf{q}}_{s_k} \\ \hat{\mathbf{q}}_{s_c}\end{Bmatrix} = \begin{Bmatrix}\hat{\mathbf{F}}_m + \hat{\mathbf{F}}^*_{ma} \\ \hat{\mathbf{F}}^*_{ea} \\ \hat{\mathbf{F}}^*_{s_ka} \\ \hat{\mathbf{F}}^*_{s_ca}\end{Bmatrix} \tag{58}$$

The modified stiffness matrices and load vectors are:

$$\begin{aligned}\hat{\mathbf{K}}^*_{mm}\left(\mathbf{q}_{s_k},\hat{\mathbf{q}}_a\right) &= \hat{\mathbf{K}}_{mm}\left(\mathbf{q}_{s_k},\mathbf{q}_a\right) - \hat{\mathbf{K}}_{mc}\hat{\mathbf{K}}_{cc}^{-1}\hat{\mathbf{K}}_{cm} \\ \hat{\mathbf{K}}^*_{me} &= \hat{\mathbf{K}}_{me} + \hat{\mathbf{K}}_{mc}\hat{\mathbf{K}}_{cc}^{-1}\hat{\mathbf{K}}_{ce} \\ \hat{\mathbf{K}}^*_{ms_k} &= \hat{\mathbf{K}}_{ms_k} + \hat{\mathbf{K}}_{mc}\hat{\mathbf{K}}_{cc}^{-1}\hat{\mathbf{K}}_{cs_k} \\ \hat{\mathbf{K}}^*_{ms_c} &= \hat{\mathbf{K}}_{ms_c} + \hat{\mathbf{K}}_{mc}\hat{\mathbf{K}}_{cc}^{-1}\hat{\mathbf{K}}_{cs_c} \\ \hat{\mathbf{K}}^*_{ee} &= \hat{\mathbf{K}}_{ee} - \hat{\mathbf{K}}_{ec}\hat{\mathbf{K}}_{cc}^{-1}\hat{\mathbf{K}}_{ce} \\ \hat{\mathbf{K}}^*_{es_k} &= \hat{\mathbf{K}}_{ec}\hat{\mathbf{K}}_{cc}^{-1}\hat{\mathbf{K}}_{cs_k} \\ \hat{\mathbf{K}}^*_{es_c} &= \hat{\mathbf{K}}_{es_c} + \hat{\mathbf{K}}_{ec}\hat{\mathbf{K}}_{cc}^{-1}\hat{\mathbf{K}}_{cs_c} \\ \hat{\mathbf{K}}^*_{s_ks_k} &= \hat{\mathbf{K}}_{s_ks_k} - \hat{\mathbf{K}}_{s_kc}\hat{\mathbf{K}}_{cc}^{-1}\hat{\mathbf{K}}_{cs_k} \\ \hat{\mathbf{K}}^*_{s_ks_c} &= \hat{\mathbf{K}}_{s_kc}\hat{\mathbf{K}}_{cc}^{-1}\hat{\mathbf{K}}_{cs_c} \\ \hat{\mathbf{K}}^*_{s_cs_c} &= \hat{\mathbf{K}}_{s_cs_c} - \hat{\mathbf{K}}_{s_cc}\hat{\mathbf{K}}_{cc}^{-1}\hat{\mathbf{K}}_{cs_c} \\ \hat{\mathbf{F}}^*_{ma} &= \hat{\mathbf{F}}_{ma} + \hat{\mathbf{K}}_{mc}\hat{\mathbf{K}}_{cc}^{-1}\hat{\mathbf{F}}_{ca} \\ \hat{\mathbf{F}}^*_{ea} &= \hat{\mathbf{F}}_{ea} + \hat{\mathbf{K}}_{ec}\hat{\mathbf{K}}_{cc}^{-1}\hat{\mathbf{F}}_{ca} \\ \hat{\mathbf{F}}^*_{s_ka} &= \hat{\mathbf{K}}_{s_kc}\hat{\mathbf{K}}_{cc}^{-1}\hat{\mathbf{F}}_{ca} \\ \hat{\mathbf{F}}^*_{s_ca} &= \hat{\mathbf{K}}_{s_cc}\hat{\mathbf{K}}_{cc}^{-1}\hat{\mathbf{F}}_{ca}\end{aligned} \tag{59}$$

In the case of short-circuited piezoelectric sensors, $\hat{\mathbf{q}}_{s_k} = \mathbf{0}$ and $\hat{\mathbf{q}}_{s_c} = \mathbf{0}$. Thus, the third and fourth lines of Eq. (58) can be neglected. On the other hand, for the open-circuit case, the induced differences of potential $\hat{\mathbf{q}}_{s_c}$ for the core piezoelectric layer can be obtained by solving the fourth line of Eq. (58). Hence, $\hat{\mathbf{q}}_{s_c}$ is written in terms of $\hat{\mathbf{q}}_m$, $\hat{\mathbf{q}}_e$ and $\hat{\mathbf{q}}_{s_k}$ as follows:

$$\hat{\mathbf{q}}_{s_c} = \hat{\mathbf{K}}^{*}_{s_c s_c}{}^{-1}\left(\hat{\mathbf{K}}^{*}_{s_c m}\hat{\mathbf{q}}_m + \hat{\mathbf{K}}^{*}_{s_c e}\hat{\mathbf{q}}_e + \hat{\mathbf{K}}^{*}_{s_c s_k}\hat{\mathbf{q}}_{s_k} + \hat{\mathbf{F}}^{*}_{s_c a}\right) \tag{60}$$

Replacing $\hat{\mathbf{q}}_{s_c}$ in the first, second and third lines of Eq. (58) yields:

$$\begin{bmatrix} \hat{\mathbf{M}} & \mathbf{0} & \mathbf{0} \\ \mathbf{0} & \mathbf{0} & \mathbf{0} \\ \mathbf{0} & \mathbf{0} & \mathbf{0} \end{bmatrix}\begin{Bmatrix} \ddot{\hat{\mathbf{q}}}_m \\ \ddot{\hat{\mathbf{q}}}_e \\ \ddot{\hat{\mathbf{q}}}_{s_k} \end{Bmatrix} + \begin{bmatrix} \hat{\mathbf{K}}^{**}_{mm}\left(\mathbf{q}_{s_k}, \mathbf{q}_a\right) & -\hat{\mathbf{K}}^{**}_{me} & -\hat{\mathbf{K}}^{**}_{ms_k} \\ -\hat{\mathbf{K}}^{**}_{em} & \hat{\mathbf{K}}^{**}_{ee} & -\hat{\mathbf{K}}^{**}_{es_k} \\ -\hat{\mathbf{K}}^{**}_{s_k m} & -\hat{\mathbf{K}}^{**}_{s_k e} & \hat{\mathbf{K}}^{**}_{s_k s_k} \end{bmatrix}\begin{Bmatrix} \hat{\mathbf{q}}_m \\ \hat{\mathbf{q}}_e \\ \hat{\mathbf{q}}_{s_k} \end{Bmatrix} = \begin{Bmatrix} \hat{\mathbf{F}}_m + \hat{\mathbf{F}}^{**}_{ma} \\ \hat{\mathbf{F}}^{**}_{ea} \\ \hat{\mathbf{F}}^{**}_{s_k a} \end{Bmatrix} \tag{61}$$

where the modified stiffness matrices and load vectors are,

$$\begin{aligned}
\hat{\mathbf{K}}^{**}_{mm}\left(\mathbf{q}_{s_k}, \mathbf{q}_a\right) &= \hat{\mathbf{K}}^{*}_{mm}\left(\mathbf{q}_{s_k}, \mathbf{q}_a\right) - \hat{\mathbf{K}}^{*}_{ms_c}\hat{\mathbf{K}}^{*}_{s_c s_c}{}^{-1}\hat{\mathbf{K}}^{*}_{s_c m} \\
\hat{\mathbf{K}}^{**}_{me} &= \hat{\mathbf{K}}^{*}_{me} + \hat{\mathbf{K}}^{*}_{ms_c}\hat{\mathbf{K}}^{*}_{s_c s_c}{}^{-1}\hat{\mathbf{K}}^{*}_{s_c e} \\
\hat{\mathbf{K}}^{**}_{ms_k} &= \hat{\mathbf{K}}^{*}_{ms_k} + \hat{\mathbf{K}}^{*}_{ms_c}\hat{\mathbf{K}}^{*}_{s_c s_c}{}^{-1}\hat{\mathbf{K}}^{*}_{s_c s_k} \\
\hat{\mathbf{K}}^{**}_{ee} &= \hat{\mathbf{K}}^{*}_{ee} - \hat{\mathbf{K}}^{*}_{es_c}\hat{\mathbf{K}}^{*}_{s_c s_c}{}^{-1}\hat{\mathbf{K}}^{*}_{s_c e} \\
\hat{\mathbf{K}}^{**}_{es_k} &= \hat{\mathbf{K}}^{*}_{es_k} + \hat{\mathbf{K}}^{*}_{es_c}\hat{\mathbf{K}}^{*}_{s_c s_c}{}^{-1}\hat{\mathbf{K}}^{*}_{s_c s_k} \\
\hat{\mathbf{K}}^{**}_{s_k s_k} &= \hat{\mathbf{K}}^{*}_{s_k s_k} - \hat{\mathbf{K}}^{*}_{s_k s_c}\hat{\mathbf{K}}^{*}_{s_c s_c}{}^{-1}\hat{\mathbf{K}}^{*}_{s_c s_k} \\
\hat{\mathbf{F}}^{**}_{ma} &= \hat{\mathbf{F}}^{*}_{ma} + \hat{\mathbf{K}}^{*}_{ms_c}\hat{\mathbf{K}}^{*}_{s_c s_c}{}^{-1}\hat{\mathbf{F}}^{*}_{s_c a} \\
\hat{\mathbf{F}}^{**}_{ea} &= \hat{\mathbf{F}}^{*}_{ea} + \hat{\mathbf{K}}^{*}_{es_c}\hat{\mathbf{K}}^{*}_{s_c s_c}{}^{-1}\hat{\mathbf{F}}^{*}_{s_c a} \\
\hat{\mathbf{F}}^{**}_{s_k a} &= \hat{\mathbf{F}}^{*}_{s_k a} + \hat{\mathbf{K}}^{*}_{s_k s_c}\hat{\mathbf{K}}^{*}_{s_c s_c}{}^{-1}\hat{\mathbf{F}}^{*}_{s_c a}
\end{aligned} \tag{62}$$

For the open circuit case, $\hat{\mathbf{q}}_{s_k}$ can be expressed in terms of $\hat{\mathbf{q}}_m$ and $\hat{\mathbf{q}}_e$ as follows:

$$\hat{\mathbf{q}}_{s_k} = \hat{\mathbf{K}}^{**}_{s_k s_k}{}^{-1}\left(\hat{\mathbf{K}}^{**}_{s_k m}\hat{\mathbf{q}}_m + \hat{\mathbf{K}}^{**}_{s_k e}\hat{\mathbf{q}}_e + \hat{\mathbf{F}}^{**}_{s_k a}\right) \tag{63}$$

Replacing $\hat{\mathbf{q}}_{s_k}$ in the first and second lines of Eq. (61) yields:

$$\begin{bmatrix} \hat{\mathbf{M}} & \mathbf{0} \\ \mathbf{0} & \mathbf{0} \end{bmatrix}\begin{Bmatrix} \ddot{\hat{\mathbf{q}}}_m \\ \ddot{\hat{\mathbf{q}}}_e \end{Bmatrix} + \begin{bmatrix} \hat{\mathbf{K}}^{***}_{mm}\left(\mathbf{q}_{s_k}, \mathbf{q}_a\right) & -\hat{\mathbf{K}}^{***}_{me} \\ -\hat{\mathbf{K}}^{***}_{em} & \hat{\mathbf{K}}^{***}_{ee} \end{bmatrix}\begin{Bmatrix} \hat{\mathbf{q}}_m \\ \hat{\mathbf{q}}_e \end{Bmatrix} = \begin{Bmatrix} \hat{\mathbf{F}}_m + \hat{\mathbf{F}}^{***}_{ma} \\ \hat{\mathbf{F}}^{***}_{ea} \end{Bmatrix} \tag{64}$$

where the modified stiffness matrices and load vectors are:

$$\begin{aligned}
\hat{\mathbf{K}}^{***}_{mm}\left(\mathbf{q}_{s_k},\mathbf{q}_a\right) &= \hat{\mathbf{K}}^{**}_{mm}\left(\mathbf{q}_{s_k},\mathbf{q}_a\right) - \hat{\mathbf{K}}^{**}_{ms_k}\hat{\mathbf{K}}^{**}_{s_k s_k}{}^{-1}\hat{\mathbf{K}}^{**}_{s_k m} \\
\hat{\mathbf{K}}^{***}_{me} &= \hat{\mathbf{K}}^{**}_{me} + \hat{\mathbf{K}}^{**}_{ms_k}\hat{\mathbf{K}}^{**}_{s_k s_k}{}^{-1}\hat{\mathbf{K}}^{**}_{s_k e} \\
\hat{\mathbf{K}}^{***}_{ee} &= \hat{\mathbf{K}}^{**}_{ee} - \hat{\mathbf{K}}^{**}_{es_k}\hat{\mathbf{K}}^{**}_{s_k s_k}{}^{-1}\hat{\mathbf{K}}^{**}_{s_k e} \\
\hat{\mathbf{F}}^{***}_{ma} &= \hat{\mathbf{F}}^{**}_{ma} + \hat{\mathbf{K}}^{**}_{ms_k}\hat{\mathbf{K}}^{**}_{s_k s_k}{}^{-1}\hat{\mathbf{F}}^{**}_{s_k a} \\
\hat{\mathbf{F}}^{***}_{ea} &= \hat{\mathbf{F}}^{**}_{ea} + \hat{\mathbf{K}}^{**}_{es_k}\hat{\mathbf{K}}^{**}_{s_k s_k}{}^{-1}\hat{\mathbf{F}}^{**}_{s_k a}
\end{aligned} \tag{65}$$

The unknown elemental internal $\hat{\mathbf{q}}_c$, sensors $\hat{\mathbf{q}}_{s_k}$ and $\hat{\mathbf{q}}_{s_c}$ DoF vectors can be computed in a post-processing calculation using Eqs. (60) and (63). To satisfy the continuity condition of the nodal electric DoFs $\hat{\mathbf{q}}_e$, the second line of Eq. (64) is to be condensed after assembling. However, the second line of Eq. (64) is valid for an element and it can be expressed as:

$$\hat{\mathbf{q}}_e = \hat{\mathbf{K}}^{***-1}_{ee}\left(\hat{\mathbf{K}}^{***}_{em}\hat{\mathbf{q}}_m + \hat{\mathbf{F}}^{***}_{ea}\right) \tag{66}$$

Replacing the latest equation into Eq. (63), the vector $\hat{\mathbf{q}}_{s_k}$ can be expressed in terms of $\hat{\mathbf{q}}_m$ and $\hat{\mathbf{q}}_a$ as follows:

$$\hat{\mathbf{q}}_{s_k} = \left(\hat{\mathbf{K}}^{**}_{s_k s_k}{}^{-1}\hat{\mathbf{K}}^{**}_{s_k m} + \hat{\mathbf{K}}^{**}_{s_k s_k}{}^{-1}\hat{\mathbf{K}}^{**}_{s_k e}\hat{\mathbf{K}}^{***-1}_{ee}\hat{\mathbf{K}}^{***}_{em}\right)\hat{\mathbf{q}}_m + \hat{\mathbf{K}}^{**}_{s_k e}\hat{\mathbf{K}}^{***-1}_{ee}\hat{\mathbf{F}}^{***}_{ea} + \hat{\mathbf{K}}^{**}_{s_k s_k}{}^{-1}\hat{\mathbf{F}}^{**}_{s_k a} \tag{67}$$

Similarly, the sensing voltage of the shear piezoelectric layers, i.e. Eq. (60), can be rewritten in terms of $\hat{\mathbf{q}}_m$ and $\hat{\mathbf{q}}_a$ as follows:

$$\begin{aligned}
\hat{\mathbf{q}}_{s_c} &= \hat{\mathbf{K}}^{*}_{s_c s_c}{}^{-1}\left[\hat{\mathbf{K}}^{*}_{s_c m} + \hat{\mathbf{K}}^{*}_{s_c e}\hat{\mathbf{K}}^{***-1}_{ee}\hat{\mathbf{K}}^{***}_{em} + \hat{\mathbf{K}}^{*}_{s_c s_k}\hat{\mathbf{K}}^{**}_{s_k s_k}{}^{-1}\left(\hat{\mathbf{K}}^{**}_{s_k m} + \hat{\mathbf{K}}^{**}_{s_k e}\hat{\mathbf{K}}^{***-1}_{ee}\hat{\mathbf{K}}^{***}_{em}\right)\right]\hat{\mathbf{q}}_m \\
&+ \hat{\mathbf{K}}^{*}_{s_c s_c}{}^{-1}\left[\hat{\mathbf{K}}^{*}_{s_c e}\hat{\mathbf{K}}^{***-1}_{ee}\hat{\mathbf{F}}^{***}_{ea} + \hat{\mathbf{K}}^{*}_{s_c s_k}\left(\hat{\mathbf{K}}^{**}_{s_k e}\hat{\mathbf{K}}^{***-1}_{ee}\hat{\mathbf{F}}^{***}_{ea} + \hat{\mathbf{K}}^{**}_{s_k s_k}{}^{-1}\hat{\mathbf{F}}^{**}_{s_k a}\right) + \hat{\mathbf{F}}^{*}_{s_c a}\right]
\end{aligned} \tag{68}$$

Considering Eqs. (67) and (68) one may notice that $\hat{\mathbf{q}}_{s_k}$ and $\hat{\mathbf{q}}_{s_c}$ are functions of $\hat{\mathbf{q}}_m$. As a result, for different values of $\hat{\mathbf{q}}_m$, different values of $\hat{\mathbf{q}}_{s_k}$ and $\hat{\mathbf{q}}_{s_c}$ will be obtained. Hence, even for one piezoelectric layer acting as sensor, different $\hat{\mathbf{q}}_{s_k}$ will be obtained for each element. However, this is not physically possible since every piezoelectric layer acting as either sensor or actuator is assigned only one sensor or actuation voltage. Therefore, if we had assembled Eq. (55), we would have considered the same $\hat{\mathbf{q}}_{s_k}$ for each element representing a specific piezoelectric layer and would have assembled this degree of freedom in a way that only one degree of freedom represents the sensor or actuator. However, Eqs. (67) and (88) are valid for an element and these equations have been used to condense the governing equation of motion of the system. Hence, in order to obtain the sensor voltage for a piezoelectric layer, Eqs. (67) and (68) should be globally assembled as follows:

$$\mathbf{q}_{s_k} = \frac{1}{\bar{n}_k}\left[\left(\mathbf{K}^{**}_{s_k s_k}{}^{-1}\mathbf{K}^{**}_{s_k m} + \mathbf{K}^{**}_{s_k s_k}{}^{-1}\mathbf{K}^{**}_{s_k e}\mathbf{K}^{***-1}_{ee}\mathbf{K}^{***}_{em}\right)\mathbf{q}_m + \mathbf{K}^{**}_{s_k e}\mathbf{K}^{***-1}_{ee}\mathbf{F}^{***}_{ea} + \mathbf{K}^{**}_{s_k s_k}{}^{-1}\mathbf{F}^{**}_{s_k a}\right] \tag{69}$$

$$\begin{aligned}\mathbf{q}_{s_c} &= \frac{\mathbf{K}^{*\ -1}_{s_c s_c}}{\bar{n}_c}\left[\mathbf{K}^{*}_{s_c m}+\mathbf{K}^{*}_{s_c e}\mathbf{K}^{***-1}_{ee}\mathbf{K}^{***}_{em}+\mathbf{K}^{*}_{s_c s_k}\mathbf{K}^{**\ -1}_{s_k s_k}\left(\mathbf{K}^{**}_{s_k m}+\mathbf{K}^{**}_{s_k e}\mathbf{K}^{***-1}_{ee}\mathbf{K}^{***}_{em}\right)\right]\mathbf{q}_m \\ &+\frac{\mathbf{K}^{*\ -1}_{s_c s_c}}{\bar{n}_c}\left[\mathbf{K}^{*}_{s_c e}\mathbf{K}^{***-1}_{ee}\mathbf{F}^{***}_{ea}+\mathbf{K}^{*}_{s_c s_k}\left(\mathbf{K}^{**}_{s_k e}\mathbf{K}^{***-1}_{ee}\mathbf{F}^{***}_{ea}+\mathbf{K}^{**\ -1}_{s_k s_k}\mathbf{F}^{**}_{s_k a}\right)+\mathbf{F}^{*}_{s_c a}\right]\end{aligned} \tag{70}$$

where $\mathbf{K}^{**}_{s_k s_k}$, $\mathbf{K}^{**}_{s_k m}$, $\mathbf{K}^{**}_{s_k e}$, $\mathbf{K}^{***}_{ee}$, $\mathbf{K}^{***}_{em}$, $\mathbf{F}^{***}_{ea}$ and $\mathbf{F}^{**}_{s_k a}$ are the global stiffness matrices and load vectors and $\bar{n}_k$ and $\bar{n}_c$ are the number of elements representing each extension piezoelectric layer and shear piezoelectric layer respectively.

Therefore, $\hat{\mathbf{K}}^{***}_{mm}\left(\mathbf{q}_{s_k},\mathbf{q}_a\right)$ can be shown as $\hat{\mathbf{K}}^{***}_{mm}\left(\mathbf{q}_m,\mathbf{q}_a\right)$ and then, Eq. (64) can be rewritten as:

$$\begin{bmatrix}\hat{\mathbf{M}} & \mathbf{0}\\ \mathbf{0} & \mathbf{0}\end{bmatrix}\begin{Bmatrix}\ddot{\hat{\mathbf{q}}}_m\\ \ddot{\hat{\mathbf{q}}}_e\end{Bmatrix}+\begin{bmatrix}\hat{\mathbf{K}}^{***}_{mm}\left(\mathbf{q}_m,\mathbf{q}_a\right) & -\hat{\mathbf{K}}^{***}_{me}\\ -\hat{\mathbf{K}}^{***}_{em} & \hat{\mathbf{K}}^{***}_{ee}\end{bmatrix}\begin{Bmatrix}\hat{\mathbf{q}}_m\\ \hat{\mathbf{q}}_e\end{Bmatrix}=\begin{Bmatrix}\hat{\mathbf{F}}_m+\hat{\mathbf{F}}^{***}_{ma}\\ \hat{\mathbf{F}}^{***}_{ea}\end{Bmatrix} \tag{71}$$

The latest equation can be globally assembled as follows:

$$\begin{bmatrix}\mathbf{M} & \mathbf{0}\\ \mathbf{0} & \mathbf{0}\end{bmatrix}\begin{Bmatrix}\ddot{\mathbf{q}}_m\\ \ddot{\mathbf{q}}_e\end{Bmatrix}+\begin{bmatrix}\mathbf{K}^{***}_{mm}\left(\mathbf{q}_m,\mathbf{q}_a\right) & -\mathbf{K}^{***}_{me}\\ -\mathbf{K}^{***}_{em} & \mathbf{K}^{***}_{ee}\end{bmatrix}\begin{Bmatrix}\mathbf{q}_m\\ \mathbf{q}_e\end{Bmatrix}=\begin{Bmatrix}\mathbf{F}_m+\mathbf{F}^{***}_{ma}\\ \mathbf{F}^{***}_{ea}\end{Bmatrix} \tag{72}$$

By considering the second line of Eq. (72), $\mathbf{q}_e$ can be expressed in term of $\mathbf{q}_m$ as:

$$\mathbf{q}_e=\mathbf{K}^{***-1}_{ee}\left(\mathbf{K}^{***}_{em}\mathbf{q}_m+\mathbf{F}^{***}_{ea}\right) \tag{73}$$

So the last step of the static condensation can be performed as follows:

$$\mathbf{M}\ddot{\mathbf{q}}_m+[\mathbf{K}^{***}_{mm}(\mathbf{q}_\mathrm{m},\mathbf{q}_\mathrm{a})-\mathbf{K}^{***}_{me}\mathbf{K}^{***-1}_{ee}\mathbf{K}^{***}_{em}]\mathbf{q}_\mathrm{m}=\mathbf{F}_\mathrm{m}+\mathbf{F}^{***}_{ma}+\mathbf{K}^{***}_{me}\mathbf{K}^{***-1}_{ee}\mathbf{F}^{***}_{ea} \tag{74}$$

However, since the $\mathbf{K}^{***}_{mm}\left(\mathbf{q}_m,\mathbf{q}_a\right)$ is a function of the $\mathbf{q}_m$ vector, Eq. (74) is nonlinear and therefore, its solution is troublesome. Hence, before assembling, it needs to be linearized.

3.2. Linearization around a static equilibrium position

It is generally assumed that the nodal load vector $\mathbf{F}_m$ is a function of the known parameters vector, $\mathbf{f}$ and a function of the displacement vector $\mathbf{q}_m$, i.e. $\mathbf{F}_m=\mathbf{F}_m\left(\mathbf{q}_m,\mathbf{f}\right)$.

Suppose that the governing equations of the system due to known ${}_i\mathbf{q}_a$ and ${}_i\mathbf{f}$ is expressed as:

$$\begin{aligned}&\mathbf{M}\ddot{\mathbf{q}}_m+\left(\mathbf{K}^{***}_{mm}\left(\mathbf{q}_m,{}_i\mathbf{q}_a\right)-\mathbf{K}^{***}_{me}\mathbf{K}^{***-1}_{ee}\mathbf{K}^{***}_{em}\right)=\\ &\mathbf{F}_m\left(\mathbf{q}_m,{}_i\mathbf{f}\right)+\mathbf{F}^{***}_{ma}\left({}_i\mathbf{q}_a\right)+\mathbf{K}^{***}_{me}\mathbf{K}^{***-1}_{ee}\mathbf{F}^{***}_{ea}\left({}_i\mathbf{q}_a\right)\end{aligned} \tag{75}$$

Assume a small perturbation around a static equilibrium position for $\mathbf{q}_m$ as:

$$\mathbf{q}_m\left(x,t\right)={}_i\mathbf{q}_m\left(x\right)+\delta\mathbf{q}_m\left(x,t\right) \tag{76}$$

where ${}_i\mathbf{q}_m$ is the static equilibrium position.

Substituting Eq. (67) into Eq. (75) and using the Taylor's series expansion around the static equilibrium position ${}_i\mathbf{q}_m$ and neglecting the higher order terms, Eq. (75) can be rewritten as:

$$\mathbf{M}\delta\ddot{\mathbf{q}}_m + \left(\mathbf{K}_{mm}^{***}\left({}_i\mathbf{q}_m, {}_i\mathbf{q}_a \right) - \mathbf{K}_{me}^{***}\mathbf{K}_{ee}^{***-1}\mathbf{K}_{em}^{***} + \left.\frac{\partial \mathbf{K}_{mm}^{***}}{\partial \mathbf{q}_m}\right|_{\mathbf{q}_m = {}_i\mathbf{q}_m} {}_i\mathbf{q}_m - \left.\frac{\partial \mathbf{F}_m}{\partial \mathbf{q}_m}\right|_{\mathbf{q}_m = {}_i\mathbf{q}_m} \right)\delta\mathbf{q}_m = \mathbf{0} \tag{77}$$

Having known both vectors ${}_i\mathbf{q}_a$ and ${}_i\mathbf{q}_m$, one may easily calculate the natural frequencies around the static equilibrium position.

The eigenvalue problems of the system under open-circuit and short-circuit electric conditions may be written, respectively, as:

$$\left(-\omega_{oc}^2\mathbf{M} + \mathbf{K}_{mm}^{***}\left({}_i\mathbf{q}_m, {}_i\mathbf{q}_a \right) - \mathbf{K}_{me}^{***}\mathbf{K}_{ee}^{***-1}\mathbf{K}_{em}^{***} + \left.\frac{\partial \mathbf{K}_{mm}^{***}}{\partial \mathbf{q}_m}\right|_{\mathbf{q}_m = {}_i\mathbf{q}_m} {}_i\mathbf{q}_m - \left.\frac{\partial \mathbf{F}_m}{\partial \mathbf{q}_m}\right|_{\mathbf{q}_m = {}_i\mathbf{q}_m} \right)\varphi^{oc} = \mathbf{0} \tag{78}$$

$$\left(-\omega_{sc}^2\mathbf{M} + \mathbf{K}_{mm}^{*}\left({}_i\mathbf{q}_m, {}_i\mathbf{q}_a \right) - \mathbf{K}_{me}^{*}\mathbf{K}_{ee}^{*-1}\mathbf{K}_{em}^{*} + \left.\frac{\partial \mathbf{K}_{mm}^{***}}{\partial \mathbf{q}_m}\right|_{\mathbf{q}_m = {}_i\mathbf{q}_m} {}_i\mathbf{q}_m - \left.\frac{\partial \mathbf{F}_m}{\partial \mathbf{q}_m}\right|_{\mathbf{q}_m = {}_i\mathbf{q}_m} \right)\varphi^{sc} = \mathbf{0} \tag{79}$$

For more details on the short-circuit and open-circuit electric boundary conditions, interested readers can refer to [1].

4. Model validation

To validate the proposed FE model, two examples are studied:

I) A pined-pined laminate elastic/shear piezoelectric/elastic beam, and

II) A clamped-free laminated elastic/adhesive/extension piezoelectric beam.

The obtained results are compared to the available data in literature in order to show the degree of agreement between the proposed and the available models.

For the following two cases, since there are no piezoelectric sensors and nonlinear mechanical forces, the terms $\frac{\partial \mathbf{K}_{mm}^{***}}{\partial \mathbf{q}_m}{}_i\mathbf{q}_m$ and $\frac{\partial \mathbf{F}_m}{\partial \mathbf{q}_m}$ are vanished from Eqs. (78) and (79). Thus:

$$\mathbf{K}_{mm}^{***}\left({}_i\mathbf{q}_m, {}_i\mathbf{q}_a \right) = \mathbf{K}_{mm}^{***} \tag{80}$$

4.1. A pined-pined laminated elastic/shear piezoelectric/elastic beam

In this section, a pined-pined sandwich beam with an embedded shear piezoelectric layer is considered (Fig. 3). The results are compared with the available numerical data in [13], analytical results of [15] and Abaqus software results from [15]. The numerical results are obtained using TSDT model where the shear strain and electric field are not constant [13]. The analytical results are obtained using the classical sandwich theory with constant shear strain and transverse electric field [15].

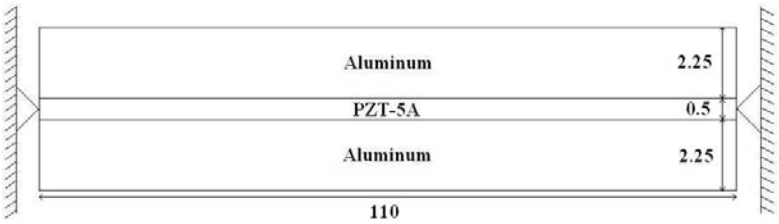

Fig. 3. A pined-pined sandwich beam with shear piezoelectric layer (dimensions are in mm)

The shear piezoelectric layer is made of PZT-5A and is sandwiched between two Aluminum layers. The material properties are as follows. For the Aluminum layers; the stiffness constants are $c_{11}^{ce} = 73$ GPa and $c_{55}^{ce} = 28.08$ GPa and the mass density is $\rho_{ce} = 2790$ kg/m^3. For the PZT-5A layer; the reduced material properties are $c_{33}^{c^*} = 60.9$ GPa, $c_{55}^{c} = 21.1$ GPa and $\rho_{cs} = 7700$ kg/m^3, the piezoelectric coupling coefficients are $e_{33}^{c^*} = 19.3$ C/m^2, $e_{15}^{c} = 12.3$ C/m^2 and the dielectric constants are $\in_{11}^{c} = 1.531\times10^{-8}$ F/m and $\in_{33}^{c^*} = 1.510\times10^{-8}$ F/m.

The first five natural flexural frequencies are obtained using the proposed model with 80 elements deployed. Presented in Tables 1 and 2, the obtained results are compared to the analytical and numerical results for short-circuit and open-circuit electric boundary conditions respectively. The results show good agreement with those reported by others.

Table 1. Comparison of analytical and numerical (Abaqus and TSDT model) results for the first five flexural natural frequencies (in Hz) under a short-circuit electric boundary condition

Mode	TSDT [13]	Analytical [14]	Abaqus[14]	Present model
1	882.7	882.7	881.6	882.0
2	3518	3524	3495	3507.0
3	7868	7904	7752	7815.2
4	13873	13988	13519	13708.0
5	21454	21734	20639	21054.1

Table 2. Comparison of analytical and numerical (Abaqus and TSDT model) results for first five flexural natural frequencies (in Hz) under an open-circuit electric boundary condition

Mode	TSDT[13]	Analytical [14]	Abaqus [14]	Present model
1	882.8	882.9	881.7	882.1
2	3520	3527	3498	3508
3	7877	7919	7765	7818
4	13901	14034	13559	13718
5	21520	21845	20729	21078

4.2. A clamped-free laminated elastic/adhesive/extension piezoelectric beam

As a second example, a piezolaminated beam with an extension piezoelectric layer is considered as shown in Fig 4.

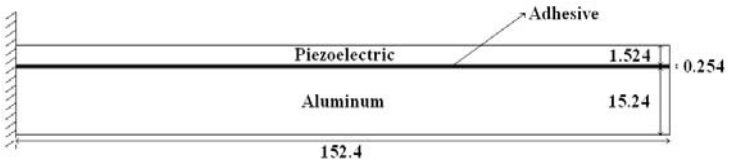

Fig. 4. A clamped-free sandwich beam with extension piezoelectric layer (dimensions are in mm)

The material properties are as follows. For the Aluminum layer; the stiffness constants are $c_{11}^{ce} = 68.97$ Gpa and $c_{55}^{ce} = 27.59$ Gpa and the mass density is $\rho_{ce} = 2769$ kg/m^3. For the adhesive layer; the Young's modulus is $c_{11}^{ce} = 6.90$ GPa and the mass density is $\rho_{ce} = 1662$ kg/m^3. The reduced material properties of the extension piezoelectric layer are $c_{11}^{k^*} = 68.97$ GPa with $\rho_k = 7600$ kg/m^3, piezoelectric coupling coefficient $e_{31}^{k^*} = -8.41$ C/m^2 and the dielectric constants are $\in_{11}^{k} = 1.505\times10^{-8}$ F/m and $\in_{33}^{k^*} = 1.150\times10^{-8}$ F/m.

For the open and closed circuit electrical boundary conditions, the first five flexural natural frequencies are computed where 14 elements are deployed. The results obtained from the proposed finite element model are compared with the results published by Krommer and Irschik [16]. Moreover, the obtained results are compared with the available data for the Timoshenko multilayer finite element model published by Trinidade, Benjeddou and Ohayon [12].

5. Numerical results

In this section, a pined-pined piezolaminated sandwich beam with extension and shear piezoelectric layers acting as actuators and sensors is considered (Fig. 5). All dimensions of the beam are in millimeters as shown in Fig. 5.

It is assumed that the extension piezoelectric layers are made of PZT-5H and their reduced material property are $c_{11}^{k_j^*} = 65.5$ GPa with $\rho_{k_j} = 7500$ kg/m^3, piezoelectric coupling coefficients $e_{31}^{k_j^*} = -23.2$ C/m^2 and the dielectric constants $\in_{11}^{k_j} = 1.505\times10^{-8}$ F/m and $\in_{33}^{k_j^*} = 1.540\times10^{-8}$ F/m. Other material properties for the shear piezoelectric and aluminum are the same as those in the previous section.

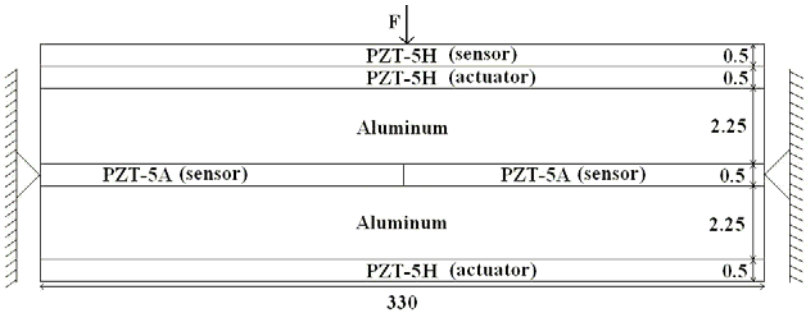

Fig. 5. A pined-pined sandwich beam with shear and extension piezoelectric layers (dimensions are in mm)

One of the extension piezoelectric layers acts as a sensor and therefore, the nonlinear effect exists here due to the von Karman's nonlinear displacement-strain relation. Since the piezoelectric sensor voltage depends on the deflection of the piezolaminated beam (see Eqs. (69) and (70)), a static external mechanical force is applied on the top surface of the piezolaminated beam.

Considering the fact that the maximum applying electric field can be about 100 kV/cm for PZT materials [17], the applied voltage to the extension piezoelectric layers is taken from 0 to -5000

Volts. Hence, by using Eq. (77), the natural flexural frequencies for different external mechanical loads at applied voltages 0 and -5000 volts are computed and presented in Table 3.

Table 3. Comparison of the nonlinear effect on the first four natural flexural frequencies and sensor voltages for different applied forces

Force (kN)	Actuator voltages	Mode 1 (Hz)	Mode 2 (Hz)	Mode 3 (Hz)	Mode 4 (Hz)	Sensor voltages (V)	
						$q_{s_{k1}}$	$q_{s_{c1}}$
$F = 20$	At 0 V	89.36	446.8	1027	1845	1399	22.06
	At -5000 V	175.6	532.6	1115	1934	458	9.61
	$\Delta(\%)$	96.51	19.20	8.57	4.82	-67.26	-56.43
$F = 10$	At 0 V	105.0	453.4	1033	1851	612.8	9.90
	At -5000 V	178.2	534.2	1117	1935	225.9	4.76
	$\Delta(\%)$	69.71	17.82	8.13	4.54	-63.14	-51.92
$F = 1$	At 0 V	114.8	458.0	1038	1856	56.32	0.93
	At -5000 V	180.5	535.7	1118	1937	22.37	0.47
	$\Delta(\%)$	57.23	16.96	7.71	4.36	-60.28	-49.46

Since the shear deformation is axisymmetric with respect to the mid-point of the beam, two shear piezoelectric layers are considered. The sensor voltages for the left shear piezoelectric layer $q_{s_{c1}}$ are tabulated in Table 3. Due to the symmetric configuration of the shear piezoelectric layers, the sensor voltage of the right shear piezoelectric layer $q_{s_{c2}}$ has an identical numeric value with the left one but with an opposite sign. The column identified by $q_{s_{k1}}$ is the voltage of the top sensor layer.

As depicted in Table 3, by increasing the applied voltage, the natural flexural frequencies are increased. This can be explained by the fact that the extension piezoelectric layers induce an axial tensile force and this tensile force stiffens the sandwich piezolaminated beam.

The voltage of the top sensor layer ($q_{s_{k1}}$) can be used to compare the axial force on the beam. From Table 3, it is obvious that by decreasing the applied force, the sensor voltage is decreased and when the sensor voltage is decreased, the nonlinear effect is less important. It is also shown that the sensor voltage of the extension piezoelectric layer is higher than the sensor voltage of the shear piezoelectric layer. Thus, for small deflections, to have a better sensitivity to deflection, one may prefer to deploy extension piezoelectric layers instead of shear piezoelectric layers.

To have a better visualization, Figs 6, 7 and 8 show the first natural flexural frequency, sensor voltages of the extension and shear piezoelectric layers for different applied mechanical forces and applied voltages respectively. As shown in Fig. 6, at different applied mechanical forces, for lower applied voltages to the extension piezoelectric actuators, the change in the first natural flexural frequency is higher than the change in the first natural flexural frequency for the higher applied voltages. This can be explained by the obtained results depicted in Fig. 7.

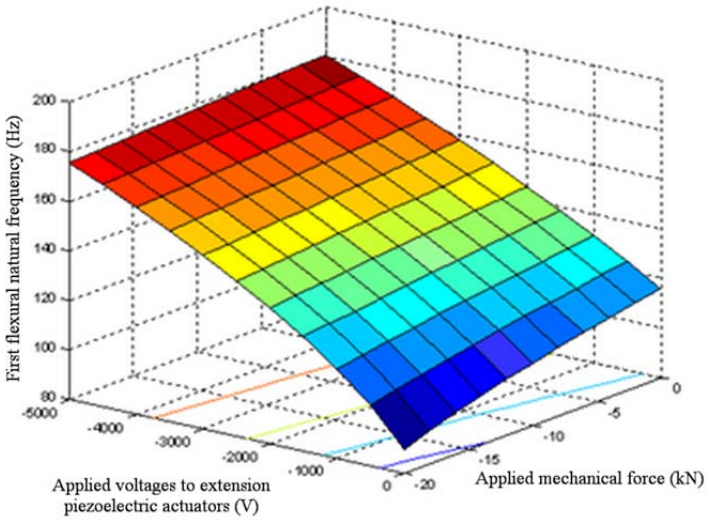

Fig. 6. First natural flexural frequency versus different applied mechanical forces and applied voltages to the extension piezoelectric actuators

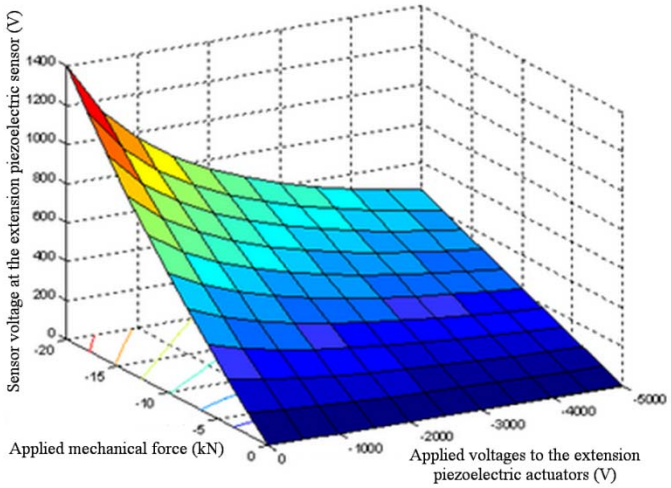

Fig. 7. Sensor voltage of the extension piezoelectric sensor versus different applied mechanical forces and applied voltages to the extension piezoelectric actuators

It shows that for lower applied voltages, the flexural stiffness is lower than the flexural stiffness for higher applied voltages. Thus, in case of applying the identical mechanical forces, for lower applied voltage, the sensor voltage of the extension piezoelectric sensor is higher than the sensor voltage for higher applied voltage.

In order to reduce the nonlinear effect, three solutions are suggested:

1) Reducing the thickness of the extension piezoelectric sensor,

2) Using a short patch of the extension piezoelectric sensor instead of a complete layer, and

3) Making the configuration symmetric according to the sensor configurations.

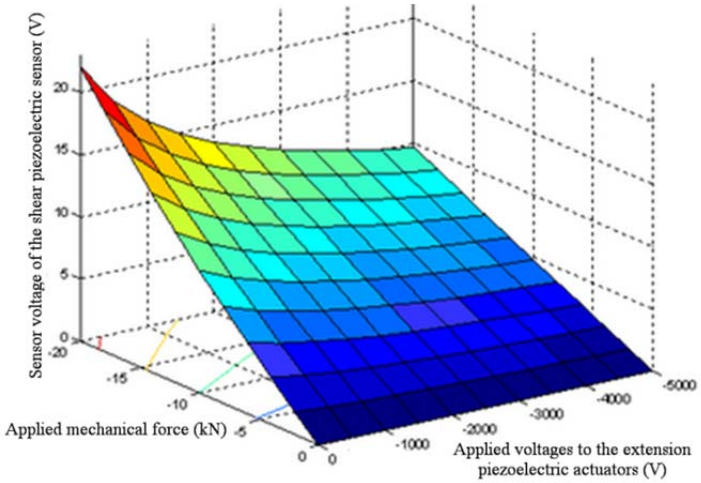

Fig. 8. Sensor voltage of the shear piezoelectric sensor versus different applied mechanical forces and applied voltages to the extension piezoelectric actuators

The last solution comes from the fact that in the case of symmetric configuration, the sensors cancel the effect of each other. For the last example, another extension piezoelectric sensor is added to the earlier configuration (i.e., Fig. 5), as shown in Fig. 9.

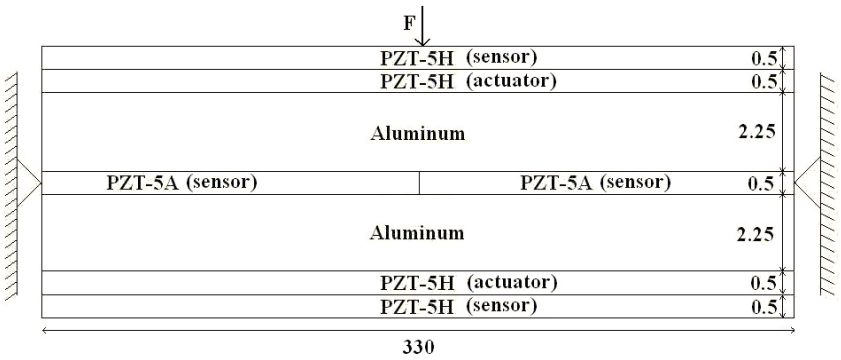

Fig. 9. A pined-pined piezolaminated beam with two symmetric extension piezoelectric sensors (dimensions are in mm)

Since the configuration of the piezolaminated beam is now symmetric according to the placement of the extension piezoelectric sensors, the nonlinear effect is nullified. For this case, the results are presented in Table 4 at 0 volt to actuator layers.

Table 4. Comparison of the nonlinear effect on the first natural flexural frequency and sensor voltage for a symmetric configuration of the sensors

Force (kN)	Mode 1 (Hz)	Mode 2 (Hz)	Mode 3 (Hz)	Mode 4 (Hz)	Sensor voltages (V)	
					$q_{s_{k1}}$	$q_{s_{c1}}$
$F=20$	124.1	497.2	1122.4	2005.4	852.7	17.27
$F=10$	124.1	497.2	1122.4	2005.4	426.3	8.64
$F=1$	124.1	497.2	1122.4	2005.4	42.63	0.86

As expected, adding another extension piezoelectric sensor stiffens the intrinsic stiffness of the piezolaminated beam. The results also indicate that for any applied mechanical force, the natural frequencies are all the same. This can be interpreted that for any applied mechanical forces, the

sensor voltages of both the top and the bottom extension piezoelectric sensors have the same magnitude with opposite sign when the top layer is in compression and the bottom layer is in tension. Therefore, these two sensors cancel out their effect and hence, the calculated natural frequencies remain unchanged for different applied mechanical forces.

6. Conclusions

In this paper, an electromechanically coupled finite element model for a piezolaminated beam was presented. For the mechanical model, the classical sandwich theory (CST) was considered with the core layers modeled according to the third-order shear deformation theory (TSDT). The face layers were modeled with the Euler-Bernoulli hypothesis. The von Karman's nonlinear displacement-strain relation was used to develop the displacement-strain relations. Using the Hamilton's principle with an extension to the piezoelectric media and governing the equation for the piezolaminated beam, it was shown that two new terms are observed for the extension piezoelectric layers due to considering the von Karman's nonlinear displacement-strain relation. One was an electromechanical stiffness-like term and the other one was a non-conservative work term. Developing the finite element (FE) model, it was shown that if the output voltage of the extension piezoelectric layer is deployed as the sensor signal, the system encounters nonlinearity and this nonlinearity in modeling of the piezolaminated beam has been pointed out for the first time. Next, the presented model was validated with two cases reported in the literature. Once the model was validated, a new case, symmetric and asymmetric configuration of a beam consisted of both extension piezoelectric actuators and sensors, was considered. It was shown that when the extension asymmetric piezoelectric sensor exists in the system, the nonlinear effect is important and the flexural natural frequencies change due to the nonlinearity.

References

[1] V.M.F. Correia, M.A.A. Gomes, A. Suleman, C.M.M. Soares, C.A.M. Soares, Modelling and design of adaptive composite structures, Computer Methods in Applied Mechanics and Engineering, 185 (2000) 325-346.
[2] M. Sunar, S.S. Rao, Recent advances in sensing and control of flexible structures via piezoelectric materials technology, Applied Mechanics Reviews, 52 (1999) 1-16.
[3] A. Benjeddou, Advances in piezoelectric finite element modeling of adaptive structural elements: a survey, Computers & Structures, 76 (2000) 347-363.
[4] A. Benjeddou, Shear-mode piezoceramic advanced materials and structures: a state of the art, Mechanics of Advanced Materials and Structures, 14 (2007) 263-275.
[5] M.A. Elshafei, F. Alraiess, Modeling and analysis of smart piezoelectric beams using simple higher order shear deformation theory, Smart Materials and Structures, 22 (2013) 035006.
[6] V. Balamurugan, S. Narayanan, A piezoelectric higher-order plate element for the analysis of multi-layer smart composite laminates, Smart Materials and Structures, 16 (2007) 2026.
[7] L.N. Sulbhewar, P. Raveendranath, A novel efficient coupled polynomial field interpolation scheme for higher order piezoelectric extension mode beam finite elements, Smart Materials and Structures, 23 (2014) 025024.
[8] O.J. Aldraihem, A.A. Khdeir, Smart beams with extension and thickness-shear piezoelectric actuators, Smart Materials and Structures, 9 (2000) 1.

[9] M.A. Trindade, A. Benjeddou, On higher-order modelling of smart beams with embedded shear-mode piezoceramic actuators and sensors, Mechanics of Advanced Materials and Structures, 13 (2006) 357-369.
[10] M.A. Trindade, A. Benjeddou, R. Ohayon, Finite element modelling of hybrid active–passive vibration damping of multilayer piezoelectric sandwich beams—part I: Formulation, International Journal for Numerical Methods in Engineering, 51 (2001) 835-854.
[11] A. Benjeddou, M.A. Trindade, R. Ohayon, New shear actuated smart structure beam finite element, AIAA journal, 37 (1999) 378-383.
[12] M.A. Trindade, A. Benjeddou, R. Ohayon, Finite element modelling of hybrid active–passive vibration damping of multilayer piezoelectric sandwich beams—part II: System Analysis, International Journal for Numerical Methods in Engineering, 51 (2001) 855-864.
[13] H. Boudaoud, A. Benjeddou, E.M. Daya, S. Belouettar, Analytical evaluation of the effective emcc of sandwich beams with a shear-mode piezoceramic core, in: Proceedings of Second International Conference on Desing and Modelling of Mechanical Systems, Monastir, Tunisia, 2007.
[14] J.N. Reddy, A simple higher-order theory for laminated composite plates, Journal of applied mechanics, 51 (1984) 745-752.
[15] M.A. Trindade, A. Benjeddou, Refined sandwich model for the vibration of beams with embedded shear piezoelectric actuators and sensors, Computers & Structures, 86 (2008) 859-869.
[16] M. Krommer, H. Irschik, On the influence of the electric field on free transverse vibrations of smart beams, Smart Materials and Structures, 8 (1999) 401.
[17] P. Muralt, Ferroelectric thin films for micro-sensors and actuators: a review, Journal of Micromechanics and Microengineering, 10 (2000) 136.